NSK Technical Journal

Motion & Control

No.10 April 2001

ISSN1342-3630

NSK

MOTION & CONTROL No.10
NSK Technical Journal
Printed and Published: April 2001
ISSN1342-3630
Publisher: NSK Ltd., Ohsaki, Shinagawa, Tokyo, JAPAN
Public Relations Department
TEL +81-3-3779-7051
FAX +81-3-3779-7431
Editor: Kyozaburo FURUMURA
Managing Editor: Yasuhiko MORITA
Design, Typesetting & Printing: Fuji Ad. Systems Corp.

Cover photos: POWERTOROS Unit Half-Toroidal CVT

NSK Technical Journal
Motion & Control
No.10
April 2001

NSK

Contents

Development of POWERTOROS Unit Half-Toroidal CVT (2)

Comparison between Half-Toroidal and Full-Toroidal CVTs

Takashi Imanishi and Hishashi Machida
Research and Development Center

ABSTRACT

There are two types of the toroidal CVT concept: a half-toroidal CVT and a full-toroidal CVT. A comparison of the following characteristics is presented in this paper: spin in the traction contact interface and axial loading force for EHL traction drives.

1. Introduction

For a long time, there have been great expectations regarding the successful application of toroidal CVT to automobiles. To this end, many such studies have been made. There are two types of the toroidal CVT concept: half-toroidal CVT and full-toroidal CVT.

The contrivance stated in U.S. patent 197 472, the earliest literature on toroidal CVTs, relates to the full-toroidal CVT. Because of their simple construction, full-toroidal CVTs were first used in automobiles during the early 1900s, and those equipped with a full-toroidal CVT were called friction drive cars. But, as indicated by this popular name, the full-toroidal CVT of those days featured direct metal-to-metal contact, which lead to low endurance. Frequent part replacement was unavoidable and burdensome. As a result, it was no longer seen after about 1915.[1] In the 1920s, General Motors started development of a traction drive lubricated with oil. This was later called a Toric transmission, and General Motors decided to start its production in 1932, but it never appeared in the market. The reason was not made known, but there is a view that the endurance of the traction transmission might not have been sufficient for automobiles. In the 1950s, Perbury Engineering took the full-toroidal CVT up anew and tested its prototypes on small vehicles. This concept has also been studied by Fellows & Greenwood et al,[2] but it has not yet been practically applied to automobiles.

The half-toroidal CVT, on the other hand, also has a long history, and its prototype embodiment was shown in the Jacob's patent in 1932. The Arter Drive, used in general industrial machines in Switzerland during the 1950s, is a half-toroidal CVT. In the 1960s, C.E. Kraus, while working for Curtis-Wright, developed a half-toroidal CVT for military vehicle applications. Kraus reported that the half-toroidal CVT was able to reduce spin loss in the traction power transmission, and that it could be applicable to automobiles. He contrived a hydraulic system capable of evenly distributing the tangential force of power rollers, and a system capable of performing stable speed changes by mechanically feeding back the tilting rotation of the power rollers. He also experimented with the performance of such systems on small cars.[3] NSK started studying the half-toroidal CVT in 1978, conducted tests of its prototypes, and completed a half-toroidal CVT—the POWERTOROS unit—by using unique materials and technologies, which were accumulated through the development of rolling bearings.[4] In November 1999, the POWERTOROS units were installed in Nissan's CEDRIC and GLORIA vehicles. Ahead of worldwide competitors, vehicles with a traction-drive type CVT have made an appearance for practical use, with the half-toroidal CVT winning the race with the full-toroidal CVT for practical application.

2. Features of a Half- and Full-Toroidal CVT

In a half-toroidal CVT, the tilting rotation center of the power rollers for transmitting power between the input and output disks is outside the center of the cavity between the disks. The cone angle, $2\theta_0$, formed by the lines connecting the traction power transmission points and the center of skewing rotation is 100°~140°. In a full-toroidal CVT, the tilting rotation center of the power rollers coincides with the center of the cavity between the disks and the angle, $2\theta_0$, is 180°. Many characteristic differences come out of this basic difference, but half-toroidal and full-toroidal CVTs have rarely been studied comprehensively. The half-toroidal CVT is given a cone angle for the purpose of minimizing spin loss in the traction power transmission zone. As a result, axial loads are generated on the power rollers, and bearings need to be added to support the axial loads. In a full-toroidal CVT, spin occurs significantly, as much as 7 times that in a half-toroidal CVT, but large-capacity bearings are not needed because no axial load is generated. As a means to produce the loading force that is necessary for traction drive, a loading cam is used for the half-toroidal CVT, and a hydraulic piston for the full-toroidal CVT.

This paper details our study made to compare the loading force generating mechanisms which are most important for the traction power transmission, as well as the effects of differences in the cone angle on the traction performance, between the half-toroidal and the full-toroidal CVTs.

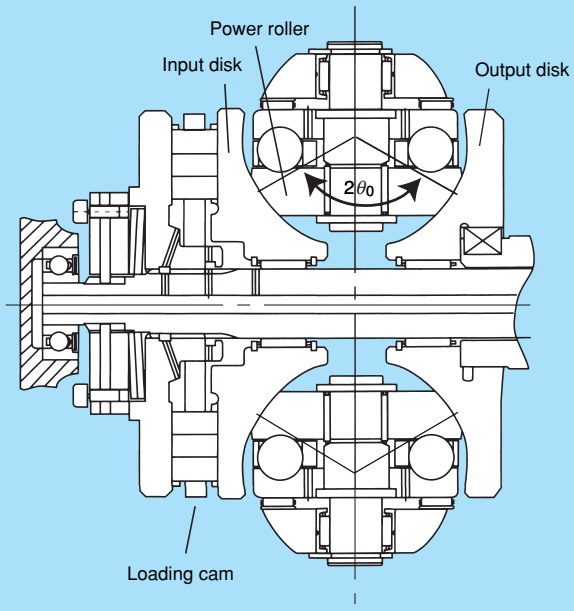

Half-toroidal CVT

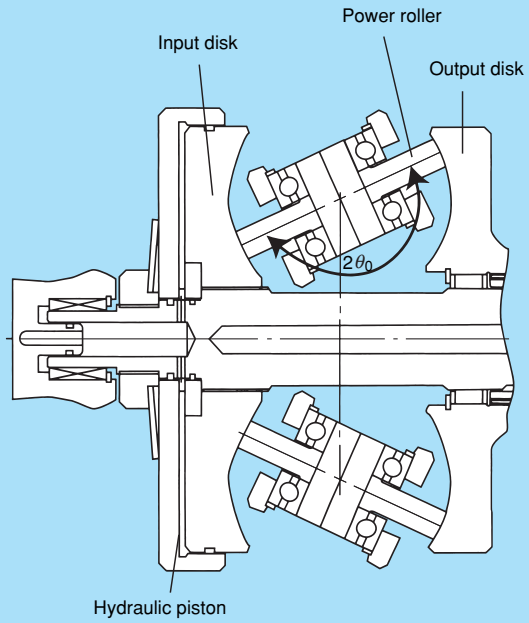

Full-toroidal CVT

Fig. 1 Half-toroidal CVT and full-toroidal CVT

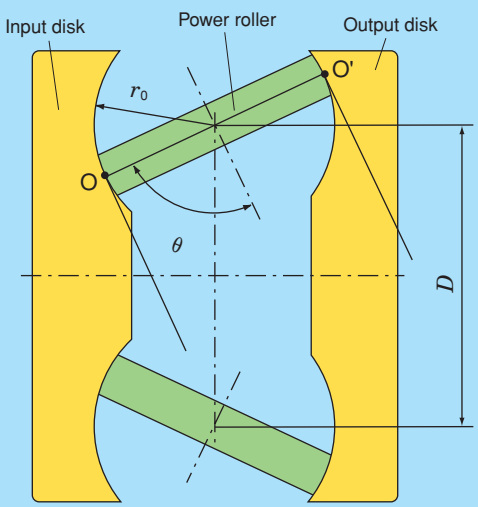

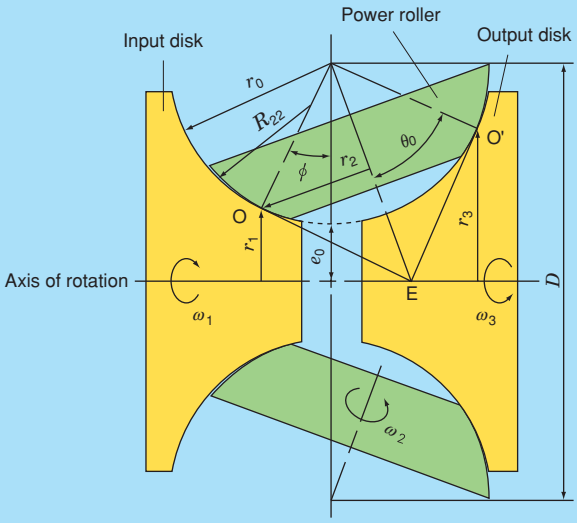

Fig. 2 Basic structures of the toroidal CVT

3. Basic Structures of Toroidal CVTs

A half-toroidal CVT and a full-toroidal CVT are illustratively shown in Fig. 1, and their basic structures in Fig. 2. The speed reduction ratio is

$$i = \frac{r_3}{r_1} \quad \ldots\ldots (1)$$

where,

$$r_1 = r_0 (1 + k - \cos\phi) \quad \ldots\ldots (2)$$

$$r_3 = r_0 \{1 + k - \cos(2\theta_0 - \phi)\} \quad \ldots\ldots (3)$$

$$k = \frac{e_0}{r_0} = \frac{D}{2r_0} - 1 \quad \ldots\ldots (4)$$

ϕ is the tilting rotation angle of the power roller. When $\theta_0 = 90°$, the CVT is full-toroidal.

4. Loading Force Generating Mechanism in Toroidal CVT

4.1 Necessary loading force for traction drive

In a traction drive system, appropriate normal force must be given to the power transmitting assembly to transmit power. The loading force needed in a toroidal CVT can be derived as follows. The input shaft torque, T_{in}, that can be transmitted by a CVT is

$$T_{in} = n \cdot r_1 \cdot F_t \quad \cdots\cdots (5)$$

n, here, is the number of power rollers. For the traction force, F_t is

$$F_t = \mu \cdot F_{cn} \quad \cdots\cdots (6)$$

From Equations (5) and (6), the necessary loading force F_{cn} at the contact point is given by

$$F_{cn} = \frac{T_{in}}{n \cdot \mu \cdot r_1} \quad \cdots\cdots (7)$$

For application of the toroidal CVT to automobiles, the loading force generating mechanism is axially attached to the back of the input or output disk, in view of available space for it. The force to be generated by the load-generating mechanism in the direction of disk rotation for the purpose of applying the loading force at the contact point is

$$F_{an} = n \cdot F_{cn} \cdot \sin\phi \quad \cdots\cdots (8)$$

By associating Equations (2) and (3) for simultaneous calculation and solving for ϕ, we get

$$\phi = \theta_0 - \sin^{-1}\left(\frac{r_3 - r_1}{2 \cdot r_0 \cdot \sin\theta_0}\right) \quad \cdots\cdots (9)$$

At the same time, we get

$$k = \frac{r_1}{r_0} + \cos\phi - 1 \quad \cdots\cdots (10)$$

$$D = 2 \cdot r_0 \cdot (1 + k) \quad \cdots\cdots (11)$$

Substituting Equation (9) in Equation (8), we get

$$F_{an} = n \cdot F_{cn} \cdot \sin\left\{\theta_0 - \sin^{-1}\left(\frac{r_3 - r_1}{2 \cdot r_0 \cdot \sin\theta_0}\right)\right\} \quad \cdots\cdots (12)$$

Now we have the necessary axial force F_{an} as a function of the half-cone angle of the power rollers. We consider here toroidal CVTs in which the radius of rotation of the contact point at the input disk, r_1, and the radius of rotation of the contact point at the output disk, r_3, are equal when the speed change is maximum, and which have a different θ_0 as shown in Fig. 3. Since the contact point rotation radii of these CVTs are made equal,

their reduction ratio widths, $i^2 = (r_3/r_1)^2$, are equal, and their disk outside diameters, $d_D = (r_3 + \alpha) \times 2$, are equal.

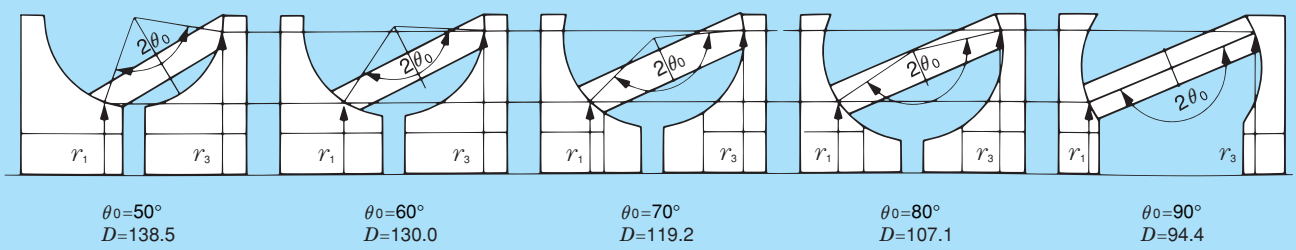

Fig. 3 Various half-cone angle of toroidal CVT

Hence, we can estimate the effect of the half-cone angle θ_0, with both the size and the reduction ratio of the reduction gear taken into account. Fig. 4 shows the necessary axial force (F_{an}) values in the entire speed reduction range (i = 2 to 0.5), obtained by calculation using θ_0 as a parameter. Table 1 lists the respective structural specifications of the CVTs. It is seen that, when the reduction ratio is maximum (i = 2), the necessary axial force for a full toroidal CVT is more than twice that for a half-toroidal CVT. This is due to the wedging effect owing to the difference in value of ϕ in Equation (8), between full-toroidal and half-toroidal CVTs, when the speed reduction is maximum. Since ϕ is smaller in a half-toroidal CVT than in a full-toroidal CVT at the time of deceleration, even a small axial loading force can produce a large contact point loading force on account of the wedge effect. In order to clearly show the effect of the geometrical difference upon the axial force, the calculations presented in this paper use a constant traction coefficient. Actually, however, considering large spin loss in the power transmitting section of a full-toroidal CVT, and a subsequent decrease in the traction coefficient, the necessary axial force may be greater.

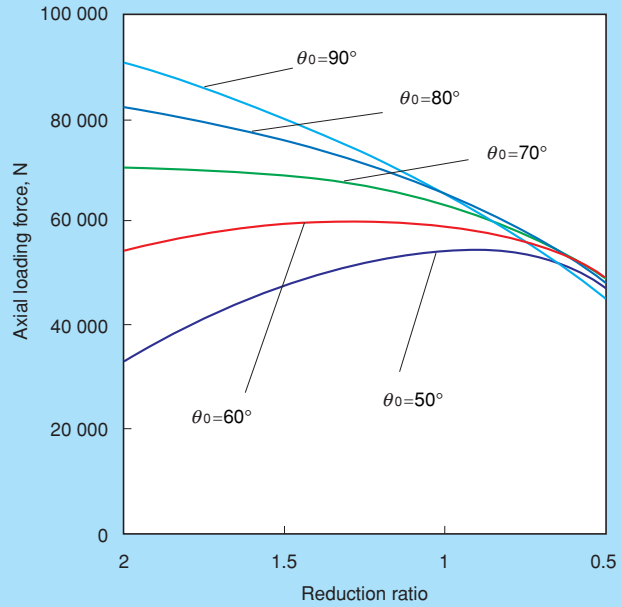

Fig. 4 Necessary axial loading force of traction drive

Table 1 Specifications of toroidal CVT

Half-cone angle θ_0, deg	Cavity diameter D, mm	Skew rotation angle ϕ, deg	Reduction ratio i
50	138.5	19.1～80.9	2.00～0.50
60	130.0	33.0～87.0	
70	119.2	45.3～94.7	
80	107.1	56.5～103.5	
90	94.4	66.9～113.2	

Common parameters:
Disk curvature r_0 = 40 mm
Input torque T_{in} = 340 N•m

4.2 Loading force generation by loading cam

The loading force generating mechanism to apply loading force necessary for the traction drive is available in two types, hydraulic and mechanical. The loading cam, which is a mechanical type, is a cam mechanism to convert the transmission torque to axial force, and is simple in structure and high in reliability, but cannot control the loading force in response to reduction ratio changes because the generated axial force is a function of the torque only. A hydraulic type can excellently control load commensurate with torque and reduction ratio changes but, for application to automobiles, it requires a powerful hydraulic pump because of dimensional limitations on the piston, and is subject to a significant power loss. In addition, it requires a hydraulic control system for the loading force control. To generate the loading force, Machida employs a loading cam for a half-toroidal CVT,[4] and Fellows a hydraulic piston for a full-toroidal CVT. On the back of the disk, both of these CVT have a mechanism to generate loading force in the axial direction.

The axial load F_{ac} generated by the loading cam is

$$F_{ac} = \frac{2\pi \cdot T_{in}}{L_c} \quad \cdots\cdots (13)$$

in which L_c is the lead of the loading cam. The loading force F_{cc} at the contact point is

$$F_{cc} = \frac{F_{ac}}{n \cdot \sin \phi} \quad \cdots\cdots (14)$$

The traction coefficient μ_c at the contact point then is

$$\mu_c = \frac{F_t}{F_{cc}} = \frac{L_c \cdot \sin \phi}{2\pi \cdot r_0 \cdot (1+k-\cos \phi)} \quad \cdots\cdots (15)$$

As seen from this equation in which ϕ is contained, the effective traction coefficient owing to the loading by the loading cam varies with the reduction ratio. The tilting rotation angle ϕ_m at which the effective traction coefficient is maximal is given by

$$\frac{d\mu_c}{d\phi} = 0. \quad \cdots\cdots (16)$$

and we get

$$\phi_m = \cos^{-1}\left(\frac{1}{1+k}\right) \quad \cdots\cdots (17)$$

The available maximum traction coefficient μ_{max} is decided by the properties of the traction oil to be used. The necessary cam lead is

$$L_c = \frac{2\pi \cdot r_0 \cdot \mu_{max} \cdot (1+k-\cos \phi_m)}{\sin \phi_m} \quad \cdots\cdots (18)$$

4.3 Use of loading cam

This subsection discusses the application of a loading cam to toroidal CVTs. In Fig. 4, the necessary axial loading force only slightly changes when θ_0= 60°, but significantly changes when θ_0 = 90°, throughout the entire reduction ratio change range. Since the axial force generated by a loading cam is a function of the input torque only and is not dependent on the reduction ratio as discussed earlier, the axial force generated by the loading cam is in excess of the axial force which needs to be generated on the acceleration side when θ_0 = 90°. At θ_0 = 60° and 90°, respectively, the necessary loading force obtained by calculating Equation (12) is shown in Fig. 5 with a red line, and that obtained by calculating Equation (13) with a blue line. It should be noted here, however, that, when θ_0 = 60°, the cam lead L_c necessary for the calculation of the cam-generated force is obtainable from Equations (17) and (18). However, when θ_0 = 90°, the cam-generated force was calculated using L_c. This was obtained by substituting the tilting rotation angle in the maximum reduction position into ϕ_m in Equation (18) since the ϕ_m obtainable from Equation (17) is outside the reduction ratio range. In a full-toroidal CVT, the excessive loading force is high on the acceleration side. This indicates that it is impractical to use a loading cam as a loading force generating mechanism in a full-toroidal CVT. The excessive loading force would shorten rolling fatigue life and require greater strength of parts resulting in heavier weight. For a full-toroidal CVT, where the necessary loading force significantly varies with reduction ratio, a hydraulic piston is suited as the loading force generating mechanism. For a half-toroidal CVT, where the necessary axial force is almost constant throughout the reduction ratio range on account of its geometrical characteristics, a loading cam is suited as the loading force generating mechanism.

5. Effects of Spinning upon Traction Performance

By calculation, we examined the effects of spinning in the traction power transmissions on traction performance. In a CVT, spinning is a gyrational sliding motion component involved in the continuous change in the radius of gyration at the traction contact point in the power transmission zone and is therefore unavoidable. Spin is transduced as loss motion, incapable of transmitting power, into heat that increases the traction oil temperature and decreases the traction coefficient. For traction drives, the knowledge of possible effects of spin upon their power transmission performance is one of the most important matters.

In this study, the effects of the half-cone angle θ_0 of the power rollers on the traction performance of a toroidal CVT were examined by calculation using Tanaka's theory.[5] Like the calculation in the discussions of the loading force generating mechanism, the calculation here was made on 5 variations of the toroidal CVT as shown in

Table 2 Calculation results

Half-cone angle	Spinning angular velocity	Maximum traction coefficient	Effective traction coefficient	Creep
θ_0 [deg]	ω_{sp} [rad/s]	μ_{max}	μ_r	C_r [%]
50	61.7	0.0697	0.0558	0.83
60	90.7	0.0656	0.0525	1.18
70	218.6	0.0521	0.0417	2.77
80	326.5	0.0452	0.0362	4.09
90	418.9	0.0410	0.0328	5.20

Common parameters:
Input speed: N_{in} = 4 000 rpm, Reduction ratio: i = 1.0, Supply oil temperature: 80°C

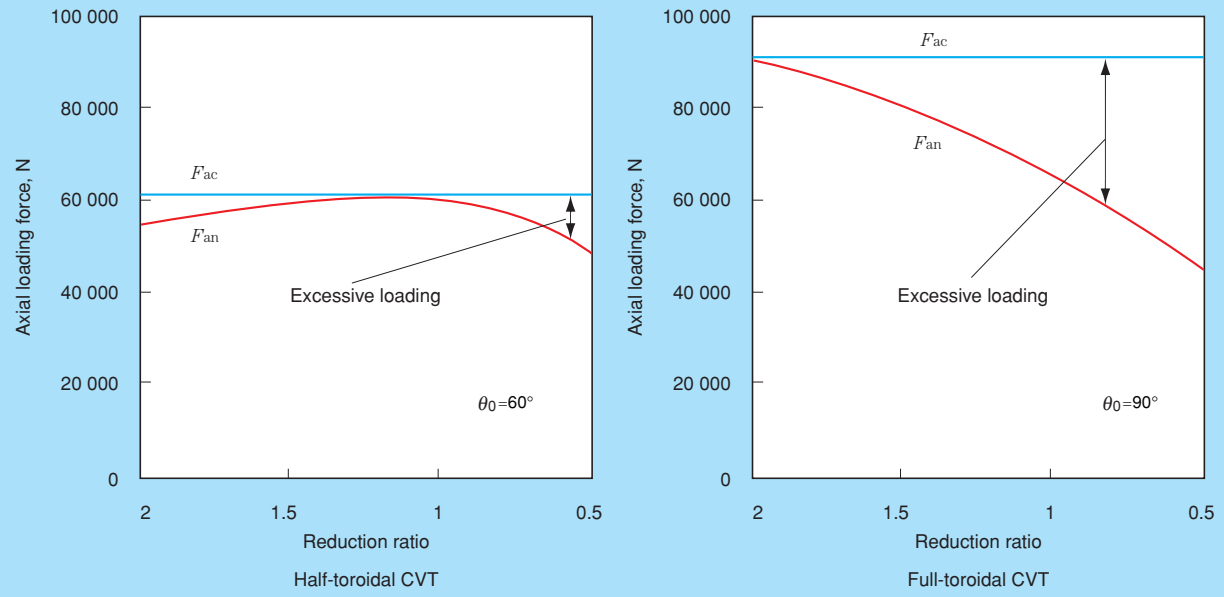

Fig. 5 Excessive loading by using loading cam

Table 2. The magnitude of the spin velocity is given by

$$\omega_{sp} = \omega_1 \sin\phi - \omega_2 \cos\theta_0 \quad \ldots\ldots\ldots\ldots\ldots\ldots (19)$$

at the input disk contact, and

$$\omega_{sp} = \omega_3 \sin(2\theta_0 - \phi) - \omega_2 \cos\theta_0 \quad \ldots\ldots\ldots\ldots\ldots\ldots (20)$$

at the output disk contact.

Table 2 lists the calculation results of the spin velocity in toroidal CVTs with a rated reduction ratio of i_{CVT} =1 and input number of revolutions of N_{in}=4 000 rpm, and with a varied θ_0 of 50° to 90°. The results show a difference up to as large as nearly 7 times. The table also lists the calculation results of the traction force coefficients, obtained by considering the traction oil as an elastoplastic fluid and by handling the effect of heating with the concept of flash temperature. A traction oil supply temperature of 80°C was used for the calculation. Also, for the purpose of this calculation, the radius of curvature of the power rollers to decide the size of an contact ellipse at the traction contact points was assumed to be 80 % of the radius of curvature of the disks. For traction curve calculation, a loading force on the contacts must be set up. Fig. 6 shows traction curve calculation results for three variations of loading force at θ_0 = 60°, which indicate that the curves vary with the loading force F_c. Since the transmission torque is assumed to be constant, the traction force F_t is constant, and the effective traction coefficient used in the power transmission is decided by the loading force F_c as shown in Equation (6). When the effective traction coefficient exceeds the maximum traction coefficient, gross slipping occurs in power transmission which disables power transmission. As seen in Fig. 6, the rate of the operating traction coefficient to the maximum traction coefficient varies from 70% through 80% to 90% as the loading force varies. These rates denote margins for gross slippage. For the purpose of this study, we obtained maximum traction curves by convergence calculation, using F_c as a parameter, and taking into account a gross slip margin of 20%, which meant that the rate of the operating traction coefficient to the maximum traction coefficient would be 80%. Fig. 7 shows the obtained traction curves at different θ_0 angles. The higher the θ_0, the less the initial slope due to the effect of the heating by spin, and also the less the maximum traction coefficient. This denotes the necessity of setting the operating traction coefficient to a small value. Table 2 summarizes the operating traction coefficients at θ_0 as well as the rates of slippage in the power transmission zone. Thus, we could quantitatively specify the relation between the half-cone angle of the power rollers, θ_0, and the traction performance.

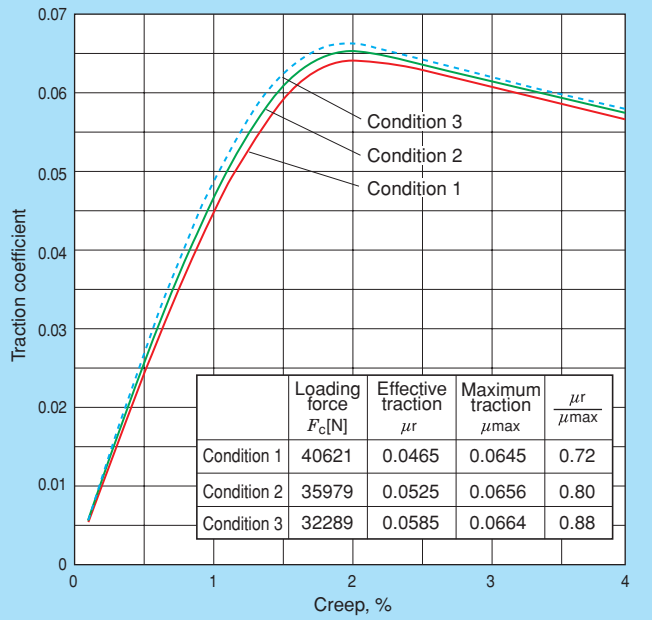

	Loading force F_c[N]	Effective traction μr	Maximum traction μmax	$\frac{\mu r}{\mu max}$
Condition 1	40621	0.0465	0.0645	0.72
Condition 2	35979	0.0525	0.0656	0.80
Condition 3	32289	0.0585	0.0664	0.88

Fig. 6 Traction curve under various F_c values

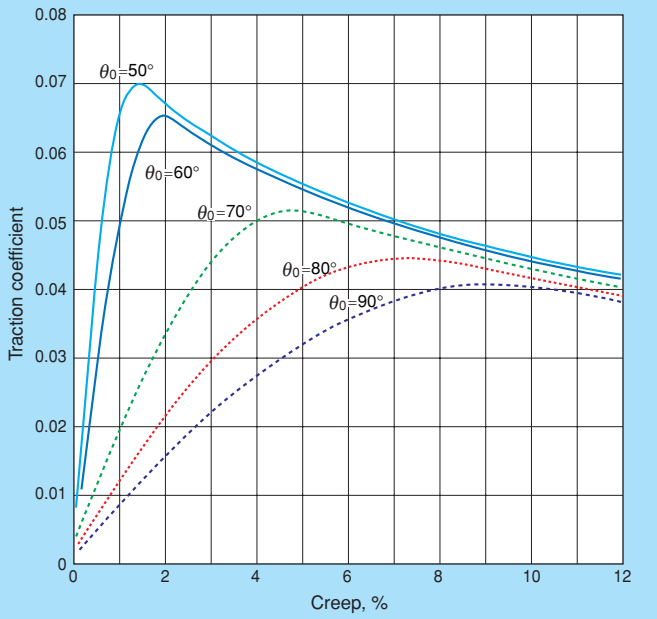

Fig. 7 Traction curve

Photo 1 Full-toroidal CVT

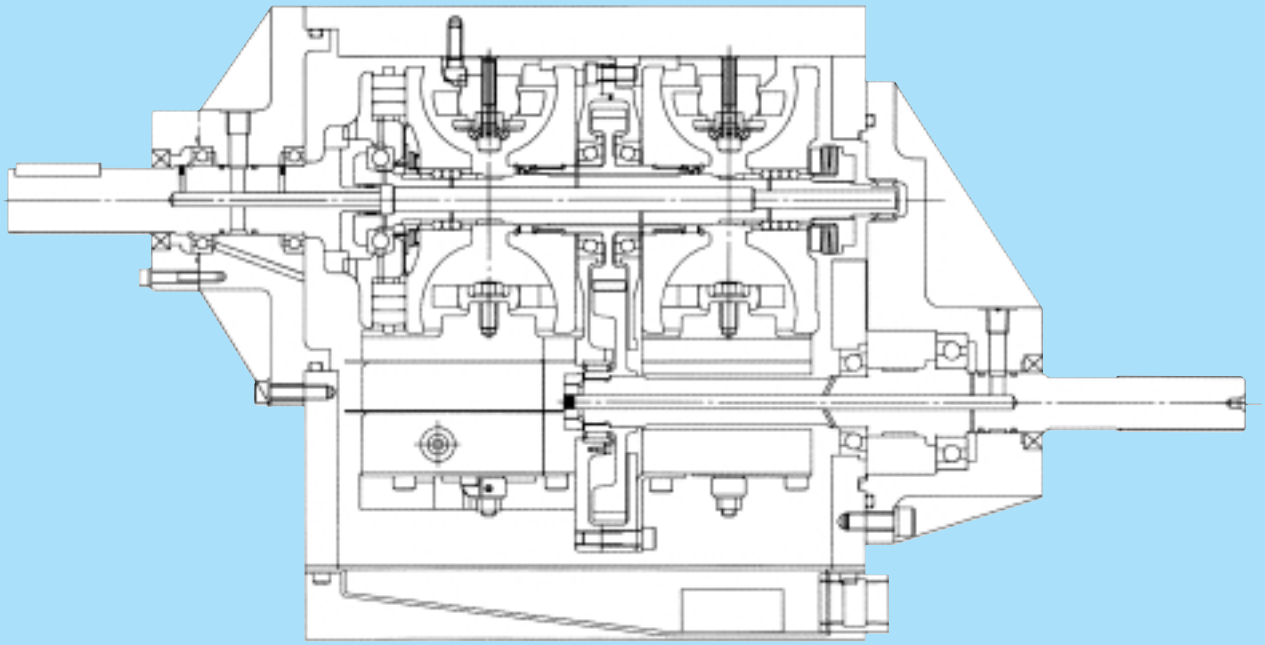

Fig. 8 Half-toroidal CVT

6. Actual Measurement of Power Transmission Efficiency of Full-Toroidal CVT

For the purpose of verifying the characteristics of a full-toroidal CVT, we built a full size full-toroidal CVT test model. Photo 1 shows its appearance, and Table 3 its main specifications. Fig. 8 illustrates a half-toroidal CVT used for comparison in the experiment, and Table 4 shows its main specifications. In consideration of their mountability in automobiles, the outside diameter of the output and input disks of both the full- and half-toroidal CVTs were made equal. Fig. 9 shows power transmission efficiency measurements as an example of the experimental results obtained with these test CVTs. The efficiency was measured between the input shaft and the output shaft of

Table 3 Specification of full-toroidal CVT

Cavity diameter	D, mm	100
Disk curvature	r_0, mm	40
Disk diameter	D_u, mm	150
Reduction ratio	i	2.00～0.50

Table 4 Specifications of half-toroidal CVT

Cavity diameter	D, mm	130
Disk curvature	r_0, mm	40
Disk diameter	D_u, mm	150
Reduction ratio	i	2.28～0.44

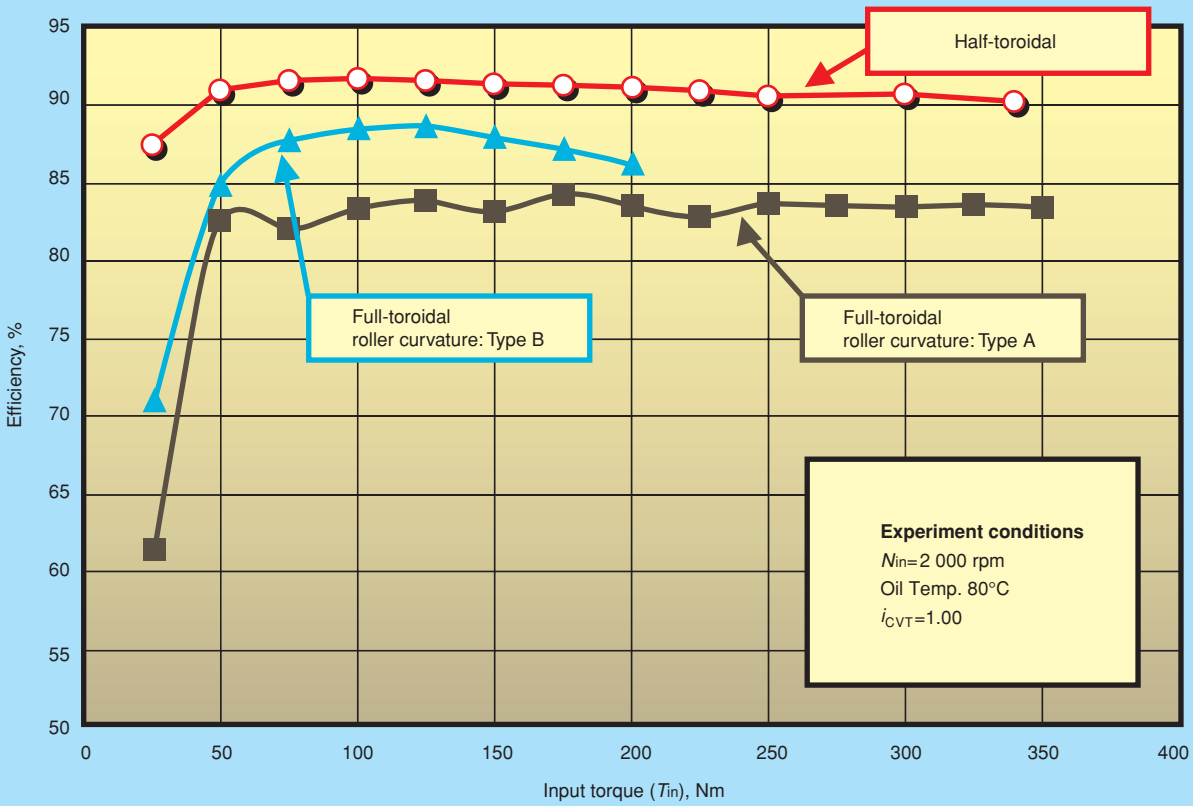

Fig. 9 Efficiency of half-toroidal and full-toroidal CVT

the tested CVTs and includes losses in parts such as gears, seals and support bearings, but does not include power loss by the hydraulic pump which was externally installed for the purpose of control, lubrication and loading force generation. The efficiency measurement was performed at the input running speed of 2 000 rpm, lubricating oil supply temperature of approximately 80°C, and the variator reduction ratio of i_{CVT} = 1.0. In consideration also of spin power loss, the traction coefficient was set to μ = 0.055 for the half-toroidal CVT, and μ = 0.035 for the full-toroidal CVT. From the half-toroidal CVT, efficiency values of approximately 90 to 92% were obtained. From the full-toroidal CVT with a
type-A roller curvature, almost flat-curve values of approximately 83 to 84% were obtained throughout the input torque range of up to 350 N·m. The roller curvature type A is designed to be smaller in curvature, to draw a smaller osculating ellipse at the traction contacts, and to have a higher surface pressure, than type B. In the CVT with the type-B roller curvature, the maximum input torque is smaller than that in the CVT with the type-A roller curvature because the surface pressure at the contacts is limited. In the experiment performed under the same conditions, a maximum efficiency of approximately 88% was obtained from the CVT with the type-B roller curvature. This higher efficiency of the type B than the type A may be explained by the smaller loss from spin due to smaller contact ellipse than the type A.

References:

1) Monsanto Magazine, Summer (1974), 14-16
2) Fellows, T.G. and Greenwood, C.J., SAE Paper 910408 (1991)
3) Kraus, J.H., Machine Design, Oct.18 (1973), 20-24
4) Machida, H. and Murakami, Y., NSK Technical Journal 669 (2000), 9-20
5) Machida, H. and Kurachi, N., Journal of JSME, 56-525, C (1990), 1282-1288
6) Tanaka, H., Journal of JSME, 53-491, C (1987), 1500-1506

Takashi Imanishi

Hisashi Machida

Development of Hub Unit Bearing with Swaging

Hirohide Ishida and Takeyasu Kaneko
Bearing Technology Center

1. Introduction

One of the key concepts relating to automobiles today is the conservation of resources and reduction in fuel consumption. In this realm, bearings for automobile wheels are required to be lighter and more compact with no less reliability. As a consequence, tapered roller bearings and single-row deep-groove ball bearings have been replaced by hub unit bearings (Fig. 1). At present, third-generation hub unit bearings (Hub III) are being utilized more extensively.

To further reduce the weight and size of Hub III designs, as well as improving reliability, NSK has developed a swaged end Hub III which is described in the following sections.

2. Structure and Features of a Hub III with Swaging

2.1 Structure of Hub III

Fig. 1 illustrates the structure of a Hub III. Both the outer and the inner rings are flanged for attachment to the vehicle. The outer ring flange is fixed to the vehicle body, and the brake assembly and the wheel are fixed to the inner ring flange.

Like a standard ball bearing, a Hub III is basically comprised of outer and inner rings, balls, and cages. More specifically, it consists of:

(1) a flanged outer ring
(2) a flanged inner ring
(3) smaller inner ring
(4) balls
(5) ball cages
(6) a clamp nut

Previously, there was a variation of the Hub III in which the flanged inner ring and another inner ring were unified, making assembly extremely difficult. Press-fitting a second, smaller inner ring onto the larger, flanged inner ring and fixing them with a clamp nut is currently the accepted traditional design (Fig. 1(c)). Functions required for this assembly include:

(1) Securely fixing the smaller inner ring with the larger, flanged inner ring.

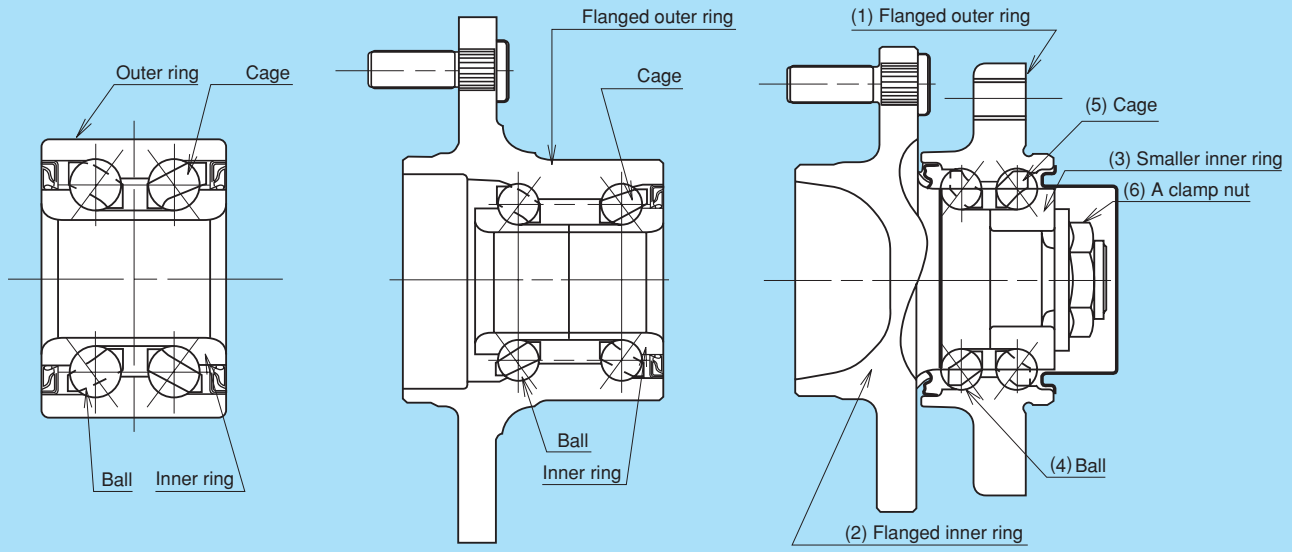

(a) First-generation hub unit (Hub I)

(b) Second-generation hub unit (Hub II)

(c) Third-generation hub unit (Hub III)

Fig. 1 Hub unit bearings

Loosening of the smaller inner ring from the flanged inner ring may allow the wheel to separate from the car body. This separation of the inner rings must be prevented.

(2) Generation of axial force to securely fasten the smaller inner ring axially:

a) prevents relative rotation (creep) between the two inner rings,

b) provides appropriate preload to improve life, rigidity and rotational accuracy, and

c) prevents separation at the mating contact face of the two inner rings when an external force is applied.

2.2 Construction and features of Hub III with swaging

In a traditional Hub III design, the two inner rings are fastened together with a clamp nut. With swaging, axial force plastically deforms the flanged inner ring to capture the smaller inner ring as shown in Fig. 2.

Elimination of the nut helps reduce the unit weight and size, and improve reliability. The same technology is applicable to both driven and non-driven wheels. Hub III applications used on driven wheels maintain a nut to provide bearing retention in combination with a CVJ as shown in Fig. 3. Fig. 4 shows the same driven wheel application using swaged bearing technology. Reliability is increased with the use of swaging as the bearing itself provides preload assurance in the event the connecting nut becomes loosened.

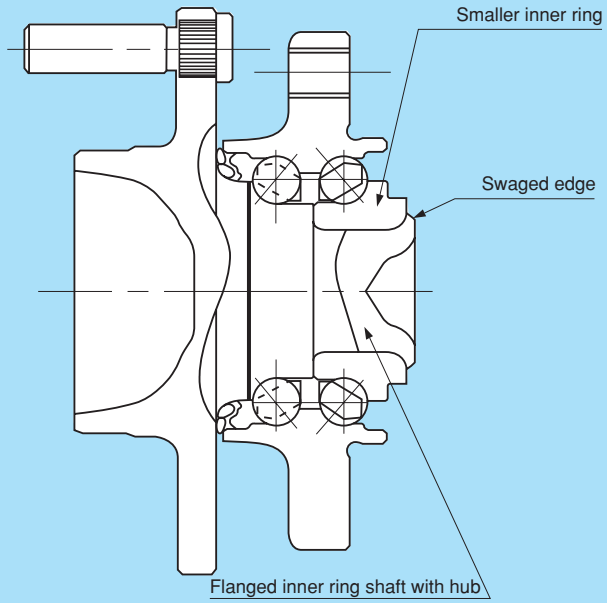

Fig. 2 Hub III with swaged edge for non-driven wheel

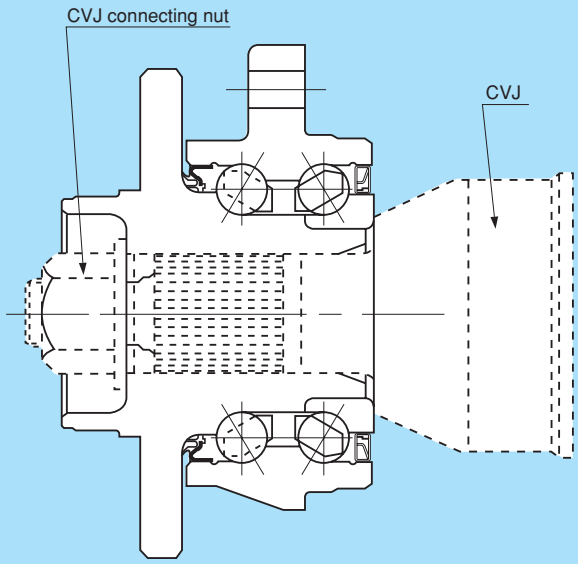

Fig. 3 Hub III (current type) for driven wheel

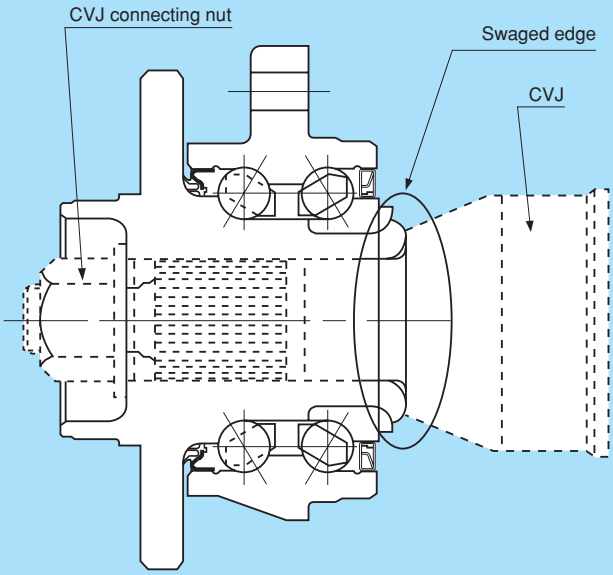

Fig. 4 Hub III with swaged edge for driven wheel

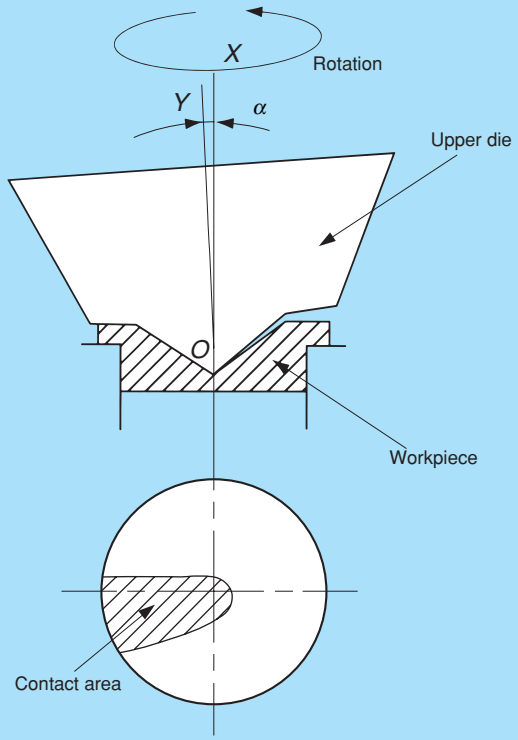

Fig. 5 Principle of rocking die forging

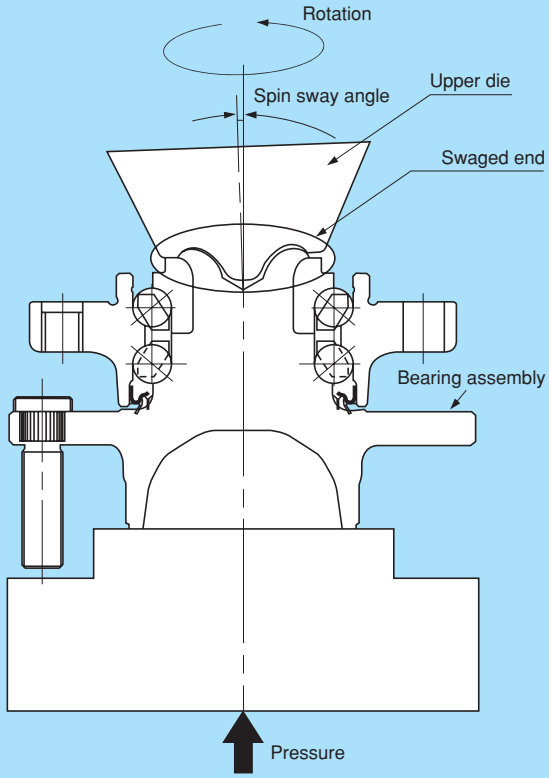

Fig. 6 Swaging

3. Swaging Process and Its Features

3.1 Swaging process

The swaging process is an applied "rocking die forging." Fig. 5 illustrates the principle of the rocking die forging. On the center point O of a workpiece, the axis OY of a conical upper die, which is tilted by an angle α from the centerline OX of the work, is turned about the OX axis. This gives rocking motion to the upper die. The lower die is pressed locally against the upper die, and the workpiece is continuously formed as the upper die continues the rocking rotation.

The NSK Hub III with swaging is an application of this rocking die forging process. Fig. 6 illustrates how a workpiece is seated between the upper and lower die sections. While the tilted upper die is rotated on a bearing assembly, pressure is applied from below to yield plastic formation at the shaft end of the flanged inner ring until it is securely fixed to the smaller inner ring.

3.2 Features

Conventional die forging affects the entire workpiece through compression and plastic formation. Therefore, a strong pressurized force is needed in working with a large object or mass. Consequently, when applied to a bearing, formation occurs beyond the localized area of concentration. Moreover, under heavy pressure, balls are pressed against the raceways possibly damaging them in the process. By contrast, the rocking die forging (swaging) locally forms an area using less pressure. By controlling localized pressure, this process is well suited for bearing assemblies.

4. Points of Development

4.1 Determination of optimum swaged edge geometry

The geometry of the swaged edge used to fasten the smaller inner ring affects the performance of the bearing as described in Section 2.

Points to be considered to determine the geometry of the swaged edge include:

- avoid concentration of residual stress
- generate sufficient axial force, and
- prevent of cracking of the swaged edge due to excessive force.

With these points in mind, we studied swaged edge

geometry.

(1) Swaged edge geometry study by strength analysis

Using pilot models in an early stage of development, we tested endurance under heavy loads. When subjected to heavy loads, the swaged edge was formed and became loose. Using FEM analysis, we then considered the cause of the loose mechanical joint. This revealed a stress concentration at the root of the swaged edge of the pilot models (Fig. 7). We also learned that maintaining the smooth bore surface of the smaller inner ring was critical throughout the swaging process (Fig. 8).

(2) Swaged edge geometry study by plastic processing analysis

Through plastic processing analysis we examined the possibility of material cracking as a result of swaging. Imparting sufficient axial force to the workpiece was also studied. Fig. 9 shows tangential stress distribution in the swaged edge portion during processing. As can be seen, the swaged edge is in a compressed state and is therefore free of cracks. Fig. 10 shows axial stress distribution after swaging. Tensile stress is produced in the flanged inner ring, while compressive stress is produced in the smaller inner ring. From this, we learned that axial force is generated by the swaging process.

The current swaged edge geometry was determined based on these analytical results.

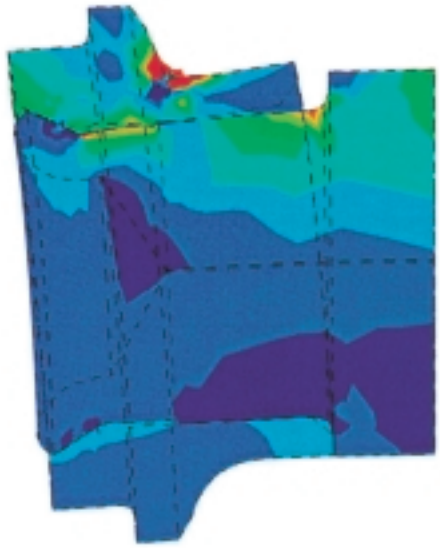

Fig. 7 Old design

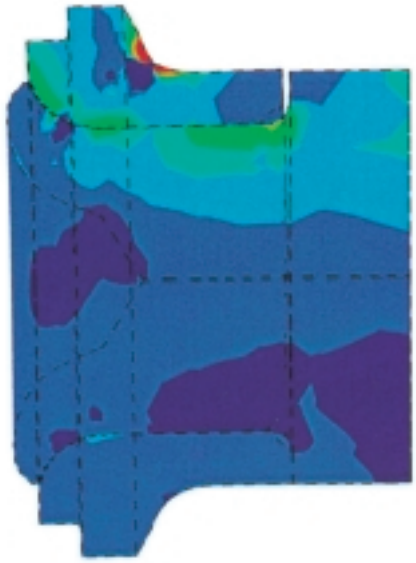

Fig. 8 Current design

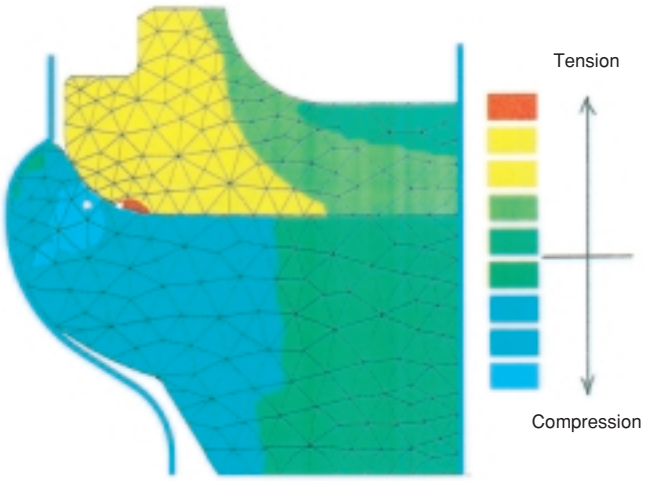

Fig. 9 Tangential stress distribution during swaging

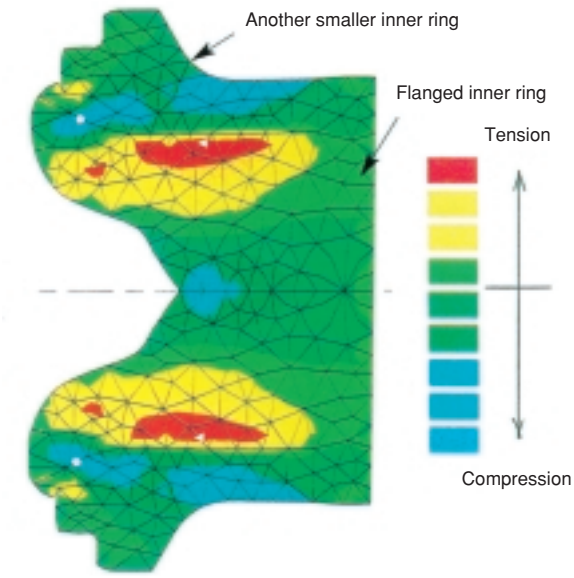

Fig. 10 Axial direction stress distribution after swaging

4.2 Swaging conditions

Important factors in determining swaging conditions include swage pressure and swage cycle time. Both swage pressure and swage cycle time need to be controlled in order to generate the appropriate axial force in order to minimize inner ring deformation. When the pressure is high, axial force is also high. Unfortunately, this leads to inner ring deformation. In an experiment, it was proven that pressure settings must be equivalent to the axial force generated by that of the clamp nut, and also, that the shortest possible swaging cycle time will ensure minimal deformation of the smaller inner ring. Fig. 11 shows the relation between the swaging cycle time and the edge (workpiece) displacement. As seen in the figure, displacement rises only slightly when the swage cycle is held for a continued period. Based on this result, we set the pressing time to a bare minimum.

4.3 Scope of heat treatment

The flanged inner ring is locally heat-treated for strength. The heat pattern, if allowed to affect the workpiece area, can cause material cracking during the swage process. For this reason, the heat zone must be precisely controlled (Fig. 12).

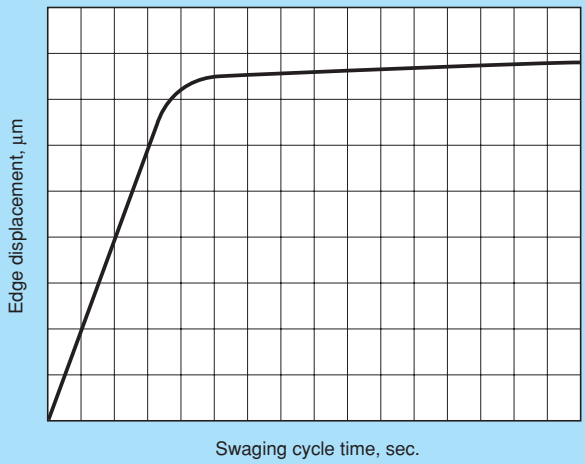

Fig. 11 Relation between time and displacement

5. Test Results

The swaged edge geometry, as determined by plastic analysis (as described in the previous section), was verified through testing. The following subsections present the test results for strength and rigidity.

5.1 Running endurance test under heavy load

This test was performed for verification of

- fatigue strength of the swaged edge, and
- inner ring resistance to creep.

Photo 1 shows the bearing after test. There was no evidence of failure due to insufficient strength of the swaged edge nor creep of the inner ring. The shaft supporting section of the tested bearing was verified to have an endurance comparable to that of a traditional Hub III bearing with clamp nut.

5.2 Static strength test

This test examined the static strength of the swaged edge. A moment load was applied until the bearing failed.

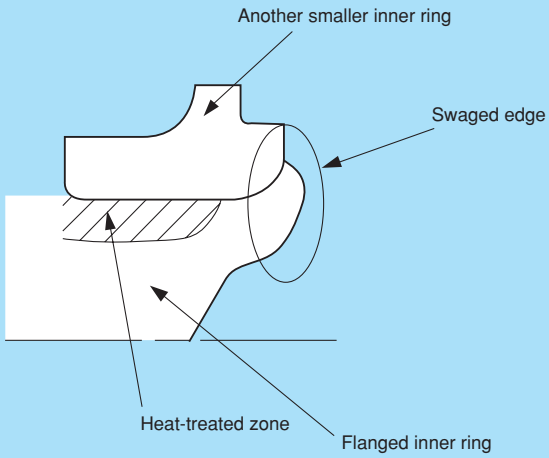

Fig. 12 Heat-treated area

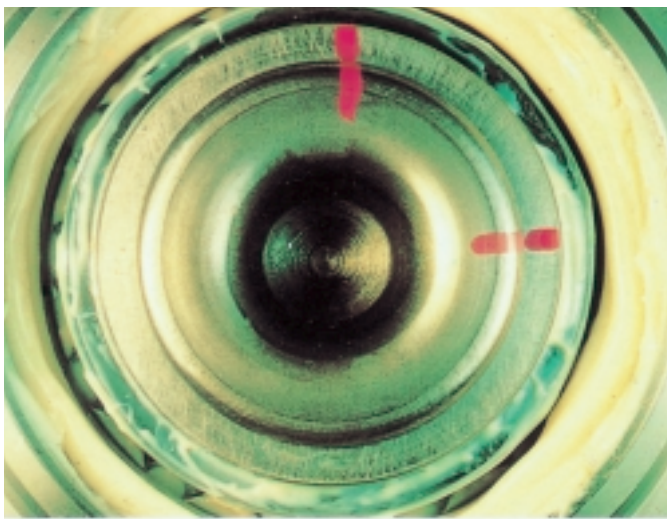

Photo 1 Condition of swaged area after heavy load endurance test

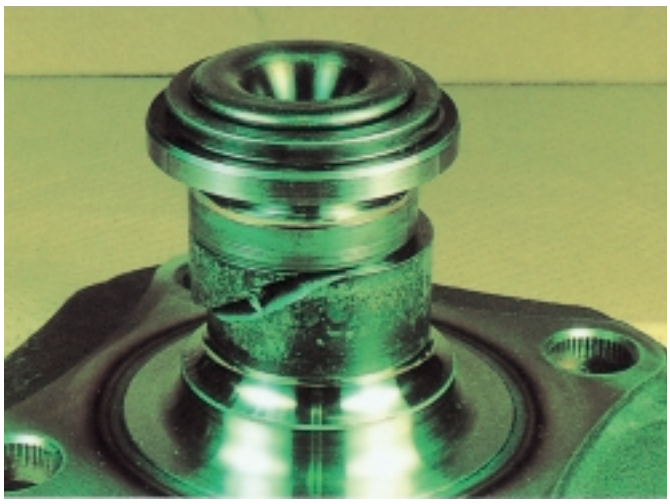

Photo 2 Condition of hub unit after static strength test (Swaged type)

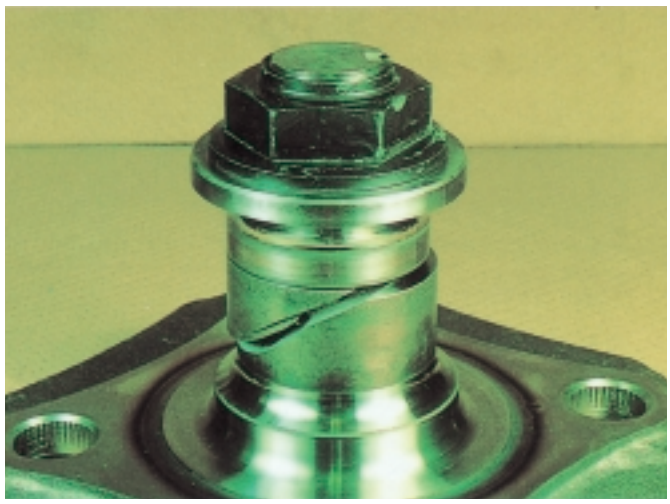

Photo 3 Condition of hub unit after static strength test (Nut type)

The mode of failure and duration until failure were noted. Photos 2 and 3 show the bearings after testing. Neither the swaged bearing nor the bearing assembled with a clamp nut failed at the fastening joint. Failure occurred in the flanged inner ring at the corner of the mating face with the smaller inner ring. The test input loads were comparable between the two bearing designs. It was also determined that the swaged edge was not the weak point of that design.

5.3 Moment load rigidity of bearing

Bearing rigidity can affect the steering stability of a vehicle under turning motion. In this test, a bearing was fixed in place as shown in Fig. 13. The relative inclination angle of the hub flange surface (A-A plane) to the outer ring flange surface (B-B plane) was measured. The rigidity of the bearing with a swaged edge was found to be equivalent to that of a bearing with a clamp nut.

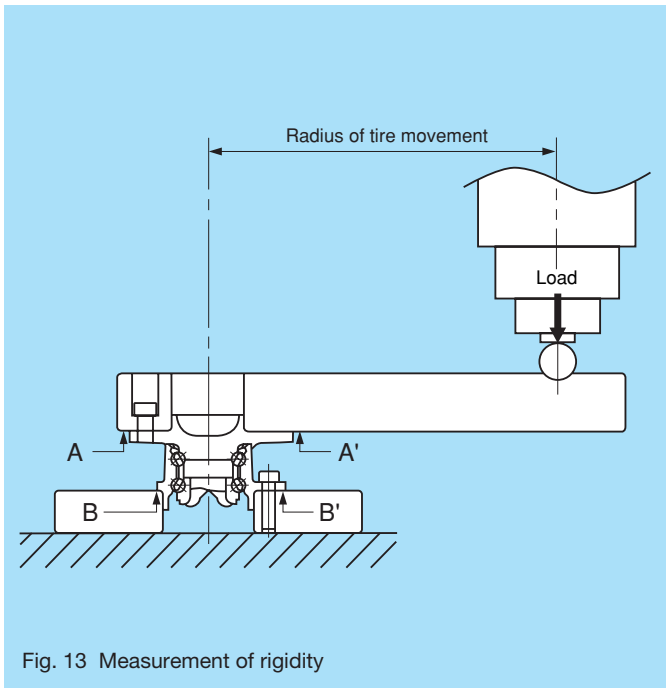

Fig. 13 Measurement of rigidity

6. Conclusion

As documented in this report, NSK's newly developed Hub III bearing with a self-retained inner ring, held by swaging, has functions equivalent to or greater than the traditional hub unit bearing with clamp nut. It has realized weight and size reductions while maintaining high reliability. It meets current market needs and is sensitive to reducing vehicle fuel consumption.

In a market that increasingly demands conservation of global resources, NSK will continue its efforts to develop products satisfying those needs.

Hirohide Ishida

Takeyasu Kaneko

An Auto-Tensioner for Timing Belts

Yoshihisa Imamura
Bearing Technology Center

1. Introduction

Timing belts are extensively used for driving the camshafts of automotive engines. To achieve a higher added value, timing belts are required to have a maintenance-free performance capability and lower noise levels.

Tensioning is an intrinsic part of the timing belt drive system and is achieved with a dedicated pulley of either a fixed or self adjusting type. Engines using a fixed-type tensioner are liable to suffer from tension variations during running. These are due to:

- elongation and wear over the lifetime of the belt
- dimensional changes due to the engine block and the belt having different coefficients of thermal expansion.

As a result, the drive is prone to noise problems and a shorter belt life under high tension. Lower tension can result in belt flapping which gives rise to unwanted noise and possible shorter life due to belt corrugation breakage.

To solve these problems auto-tensioners are used to maintain a constant tension. It is, however, being recognized that auto-tensioners having a hydraulic or friction-type damping system are not free from unstable damper characteristics and are not fully capable of ensuring an optimum tension.

NSK has recently developed an auto-tensioner having a multi-plate viscous damper and a capability of reducing belt noise.

This report describes the design, functions and features of the auto-tensioner with a unique structure.

2. Outline of NSK Auto-Tensioner for Timing Belts

2.1 Design

Fig. 1 shows an auto-tensioner assembly and Photo 1 shows the actual product. The center of the tensioner bearing is offset from the center of displacement and this positional change acts to adjust the belt tension. The tension is given by a tensile coiled spring or a twisted coil spring. One end of the spring is attached to the adjustable assembly and the other end to a fixed point such as the engine block.

The multi-plate damper is located to encompass the center of rotation and provides resistance proportional to the speed of the sub-assembly's movement.

Because of this arrangement, the tensioner follows,

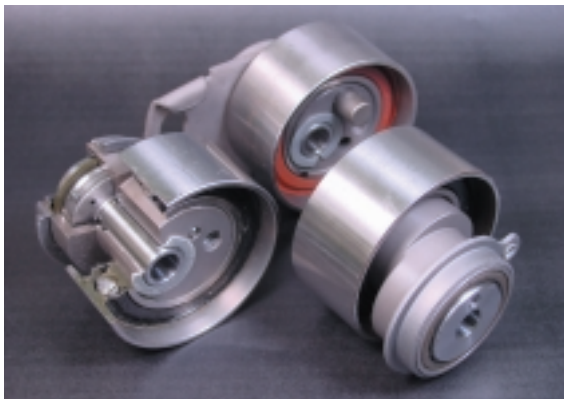

Photo 1 NSK auto-tensioners for timing belts

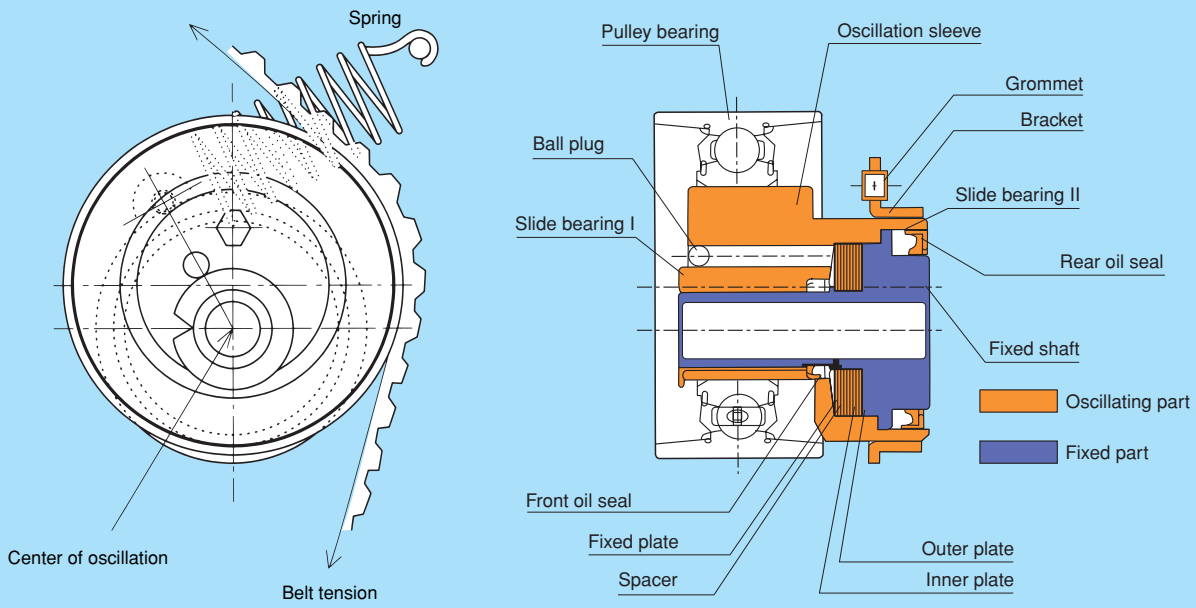

Fig. 1 Construction of NSK auto-tensioner for timing belts

without resistance, the slow tensional variations such as those due to belt elongation and temperature change. It also, however, resists movements caused by the high-frequency tensional variations coming from the engine.

The multi-plate damper of this unit uses the viscous resistance of oil contained between the inner and outer plates which are fixed to the shaft and sleeve respectively. This oil is a highly viscous silicone type whose viscosity varies only slightly with temperature. The gap between the plates is determined by the difference between outer plate thickness and the inner plate spacer.

The damper capacity depends on the number of these plates chosen, the set gap between the plates and the oil viscosity.

2.2 Features

This auto-tensioner has the following features:

(1) A compact design, where the center of the tensioner oscillation is within the bearing itself; this requires only a small space envelope.
(2) This auto-tensioner can replace an existing tensioner because the unit requires a simple screw attachment and a spring locating point.
(3) Since this auto-tensioner utilizes the viscous resistance of a fluid, it gives a large resistance to high-frequency tensional variations and minimizes belt flapping. Also, since it is free from sharp changes in resistance and damper position, it can effectively control belt tension variations even when the engine is running.
(4) Desired damper capacity is easily available by the number of plates incorporated.
(5) Damper capacity does not significantly vary with age or usage.

3. Functions and Characteristics

3.1 Absorbing fluctuating tension forces

Fig. 2 shows measurements of tensioner bearing displacements under engine block temperature variations.

According to the engine block temperature rise the tensioner bearing retracts to maintain the belt tension at a constant level.

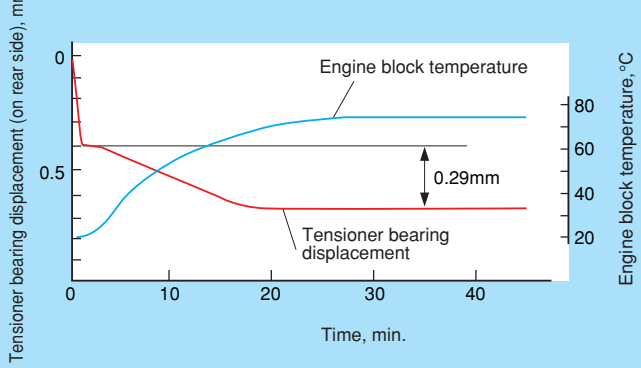

Fig. 2 Displacement of tensioner bearing

Belt tension variations measured at the same time are shown in Fig. 3. These variations were directly measured between the camshafts, with the engine being stationary.

The belt tension noticeably increases when a fixed tensioner is used but remains at almost a constant level with only a slight increase due to the elongation of the tension setting spring when the unit is running.

3.2 Characteristics of multi-plate viscous damper

The damper in the tensioner bearing utilizes the viscous resistance of a high-viscosity silicone oil contained in between the oscillating outer plate and the fixed inner plate. This viscous resistance is represented by a model shown in Fig. 4. The torque T is given by:

$$T = \int_{r_1}^{r_2} r\mu \frac{(2\pi r dr)(\omega r)}{h}$$

$$= \frac{2\pi\rho\nu}{h} \frac{(r_2^4 - r_1^4)}{4} \omega \quad \ldots\ldots\ldots\ldots\ldots\ldots (1)$$

where ρ is the density of silicone oil, ν is the kinematic viscosity, h is the gap between plates, r_1 and r_2 are inside diameter and outside diameter of the plates, and ω is relative angular velocity.

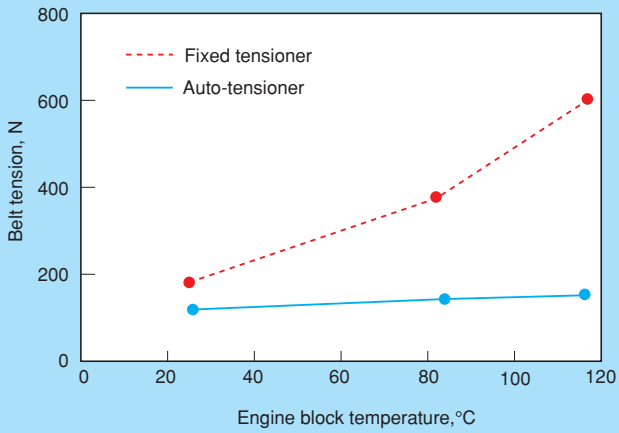

Fig. 3 Belt tension vs. temperature

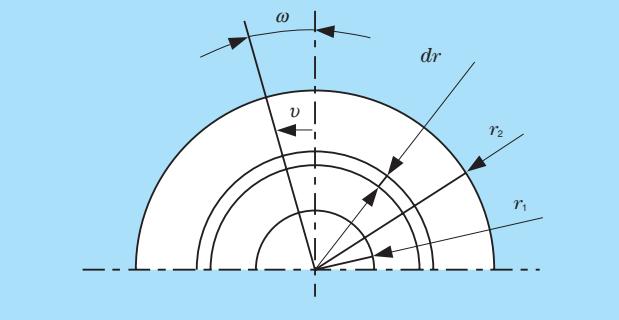

Fig. 4 Resistance of silicon oil between two parallel plates

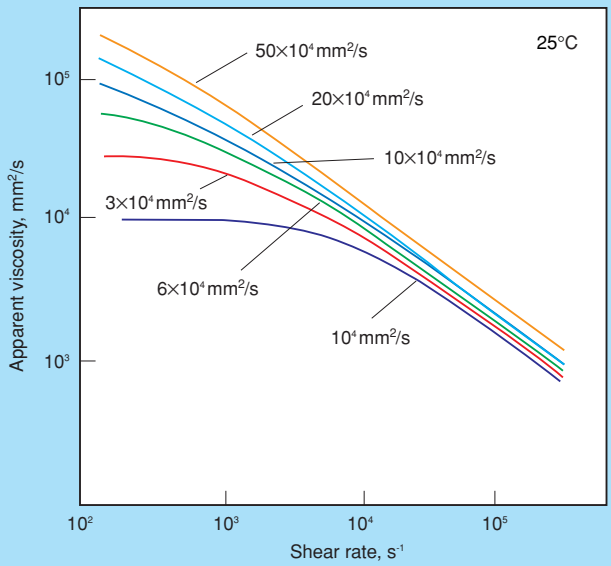

Fig. 5 Characteristics of silicon oil for shear rate

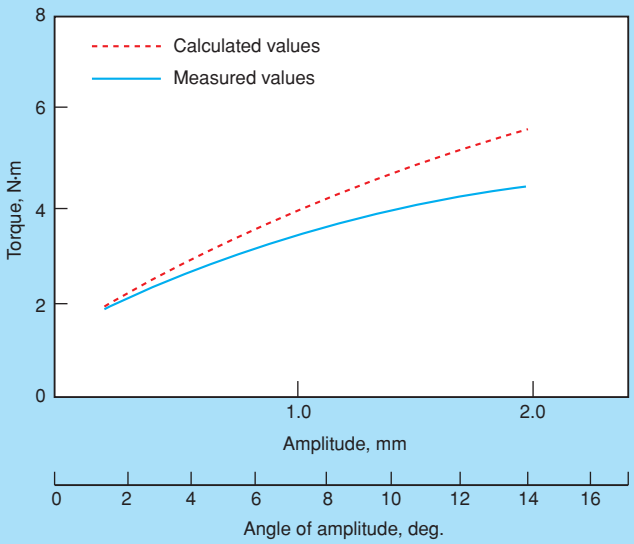

Fig. 6 Characteristics of damper for vibration amplitude

High-viscosity silicone oil, however, has a property where its apparent viscosity is subject to reduction by shearing and this needs to be taken into account. The reduction in apparent viscosity is correlated with shear rate which is determined by the relative velocity and the gap between the plates, as shown in Fig. 5. The reduction in apparent viscosity is, however, a temporary phenomenon of molecular orientation caused by shearing force and is not one caused by oil deterioration through mechanisms such as molecular chain breakage.

Fig. 6 shows torque values obtained by calculation (based on Equation (1)) with this reduction in apparent viscosity in the damper taken into account, along with those obtained by actual measurement. The measurement was performed at the same temperature.

The damper capacity slightly disagrees with the results of calculation in which the reduction in apparent viscosity caused by shear rate is taken into account. Consequently, the results should be reflected in design specifications.

3.3 Operating characteristics

The NSK auto-tensioner follows slow tensional variations without resistance. For high-frequency variations in tension caused by rotational torque variations of the camshaft and angular velocity variations of the crankshaft, a damper is incorporated for the purpose of suppressing its attempts to follow them, as previously described.

Fig. 7 shows a model of the displacement (or oscilation) amplitude.

As seen in this figure, m is oscillation inertia, c is viscosity reduction coefficient, k is spring constant, f is frictional force, and $F(t)$ is belt tension input to the tensioner bearing.

The belt tension in this model is expressed as:

$$m\ddot{x} + c\dot{x} + kx \pm f = F(t) \quad \ldots\ldots\ldots\ldots\ldots\ldots\ldots\ldots (2)$$

$F(t)$, however, is a variable load working in one direction only. For $F(t)$, the tensioner bearing is balanced mainly by c and k but, since k needs to be minimized to reduce belt tension variations to levels as low as possible, c is dominant.

If c is insufficient, the tensioner bearing response to variation components of high order will cause wide oscillations.

Tensioner bearing movements of large amplitude are desirable from the viewpoint of the balance of forces but can cause high noise and belt flapping which results in high belt tension and are therefore not desirable.

Alternatively, if c is excessively high, the assembly may oscillate with a small amplitude but may not be able to fully follow variations of the load and may be balanced by belt tension at points unintended in the original design resulting in increases in the belt tension.

Hence, it is important to control the assembly's movements to within a tolerable range to prevent such undesirable instances.

Thus, considering the foregoing discussion, it is possible to design an auto-tensioner suited for a particular engine specification by appropriately setting up c and kx.

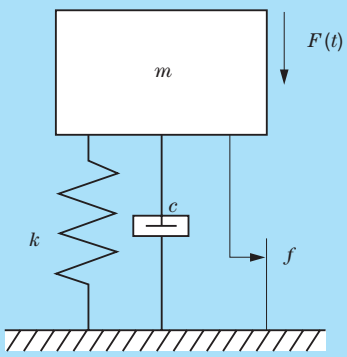

Fig. 7 Vibration model

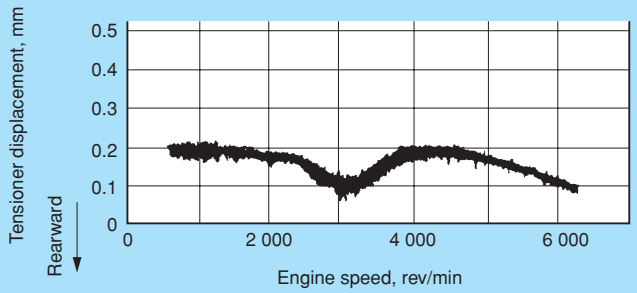

Fig. 8 Example of vibration characteristics of tensioner tested on an engine

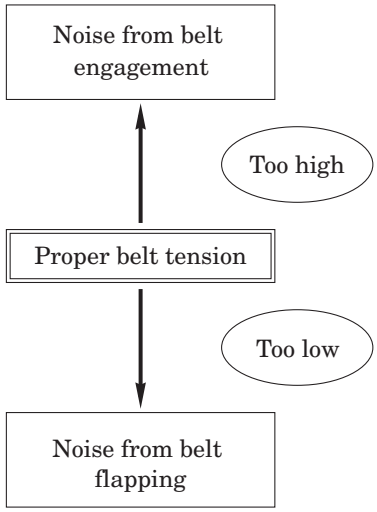

Fig. 8 shows an example of movements of an auto-tensioner design considering the above factors and mounted in an actual engine.

3.4 Damper characteristic for dynamic belt tension

The results of auto-tensioner tests on actual engines indicate that noise from the timing belt originates chiefly from the engagement of the timing belt teeth with the pulley teeth. This noise of the teeth engagement is closely related with the belt tension during engine operation. The higher the belt tension operation, the larger the teeth engagement noise.

To minimize the timing belt noise, therefore, it is necessary to control the belt tension to the lowest possible level at which the belt will not flap throughout the engine operational range. Fig. 9 shows maximum values of the dynamic tension of a timing belt under an auto-tensioner, as measured on an actual engine.

As seen in this figure, the use of this design enables control of the dynamic reaction by presetting the belt tension to within a much narrower range than when a fixed tensioner is used.

Another feature of the variable damper capacity is by selection of an appropriate number of damper plates. This

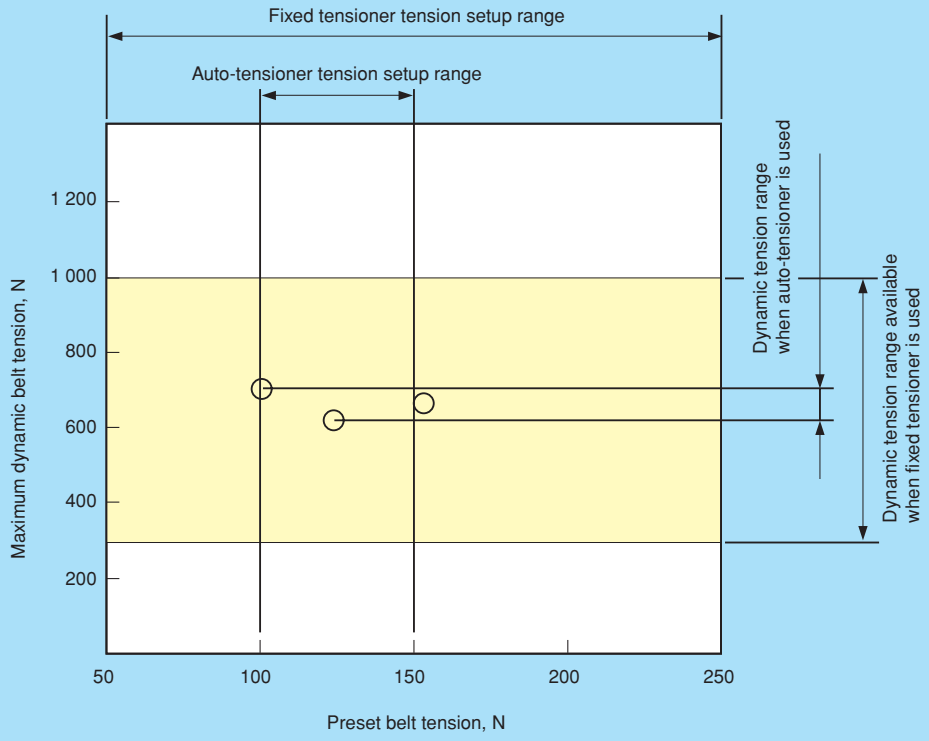

Fig. 9 Example of engine timing belt dynamic tension

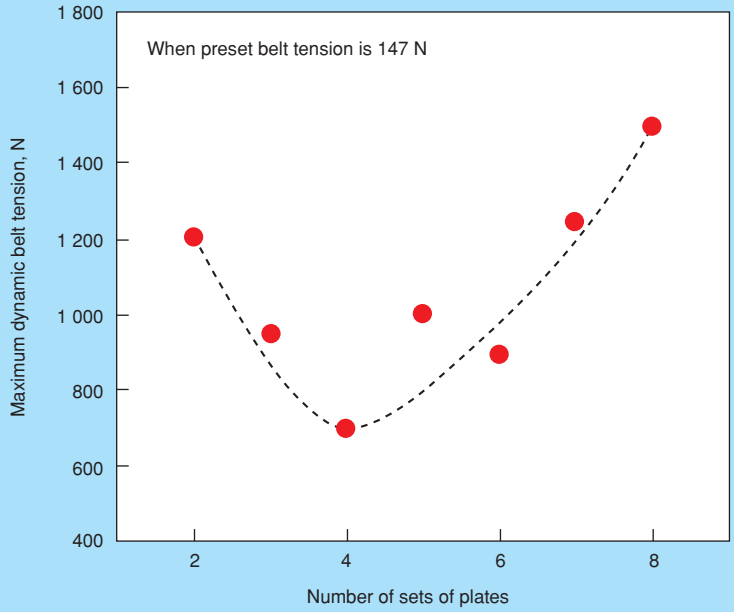

Fig. 10 Relation between damper capacity and belt tension

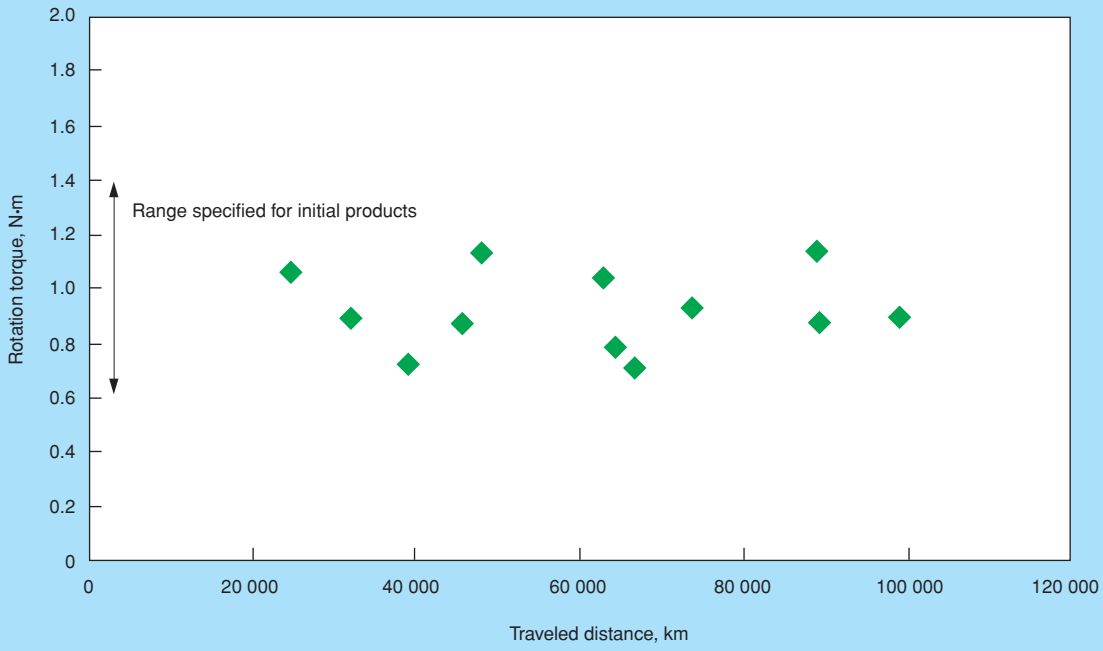

Fig. 11 Aging of damper

feature enables fine adjustment of the belt tension, as well as the tuning of the damper capacity, without requiring alteration of the installation space previously decided in the design and engineering process.

Fig. 10 shows the relation between the number of sets of the preset damper plates (the damper capacity) and the timing belt tension, verified on actual engines.

In this case, the belt flapping and belt engagement noise are minimal to indicate an optimum specification when the number of sets of damper plates is 4.

3.5 Damper aging characteristic

Fig. 11 shows the evaluation results of the NSK auto-tensioner damper aging characteristic measured on actual vehicles in terms of distance traveled.

As is obvious from this figure, the damper capability remains almost constant throughout operation over a long distance, showing little degradation due to aging.

This advantageous characteristic is due to the damper mechanism which utilizes the shearing force of oil to prevent direct contact of component parts and maintains stable tension adjustment and noise restraining capabilities over a long service period.

4. Conclusion

The foregoing sections reported the functions and characteristics of the NSK auto-tensioner having a multi-plate viscous damper for engine timing belts.

This auto-tensioner is recognized as a functional part having excellent performance and capable of providing for low noise, light weight, and good maintainability that give tangible benefits to engine timing belts and is extensively used in various automotive engines.

Efforts are continuing to pursue and improve the characteristics with the view to further developing optimum design that can enhance the performance and reliability of, and added value to, current and future engines.

Yoshihisa Imamura

Development of High-Speed Cylindrical Roller Bearings for Machine Tools

Yasushi Morita and Yukio Ohura
Bearing Technology Center

ABSTRACT

Recently Japanese machine tool manufacturers have been keen to improve and develop their machines with better productivity. That is why Japan maintains its No.1 position in world production of machine tools. As for high productivity, the spindle speed of the machining center is increasing year by year. Lathes are also becoming increasingly multi-functional to meet the requirements of the market. The trend for high-speed spindles is to integrate the motor into the spindle. Therefore, several customers are waiting for extra high-speed cylindrical roller bearings to simplify the spindle structure. NSK has been developing extra high-speed cylindrical roller bearings with robust design. This paper reports on such development, test results, and makes recommendations.

1. Introduction

Japanese machine tool manufacturers place their main effort on high-efficiency and high-accuracy machine tools as distinguished from low-priced ones. Japan ranks top in the world in terms of machine tool output. Japanese manufacturers maintain this position by constant effort for improvement and innovation.

Recently, emphasis has been placed on high efficiency and high reliability. Various improvements have been made to achieve this. Requirements for higher speed performance of machining centers are increasingly strict. In the machining of aluminium alloys in the aerospace industry, for instance, there is actually a requirement for 3 000 000 $d_m n$ (where d_m = pitch circle diameter of a bearing in mm and n = speed in rev/min).

In the current marketplace for lathes, there is a trend towards small-batch production of a large variety of configurations with short-term delivery to match the constantly evolving Japanese economy. To achieve more complex capabilities some lathes have an additional sub-spindle equal to the spindle of a current machining center. Bearing manufacturers are required to provide new products and technical support to meet such changes in demand.

To appropriately deal with these rapid changes, NSK has developed the ROBUST series of angular contact ball bearings. We exhibited them at JIMTOF (a machine tool fair in Japan) held in 1998 and launched them onto the market. At the JIMTOF held in November 2000, NSK also proposed a ROBUST series of cylindrical roller bearings. This paper describes them.

2. Change in Bearing Operating Environment

The type of drive featured on spindles of Japanese machine tools in the mainstream has been changing over the last few years. It has moved from belt driven to an integral motor, which can achieve higher-speed and high-efficiency performance. This change has been in answer to the problems of power loss and slip of the driving belt and vibration.

As a result, spindle construction has undergone significant changes. One of these is due to the presence of an integral motor acting as a heat source within the spindle. This tends to cause a temperature difference between the spindle and the housings and a subsequent stress increase in the bearings. Consequently, the bearings are liable to seize. This change necessitated the development of a bearing system capable of dealing with greater thermal effects.

NSK developed the ROBUST angular contact ball bearing (BNR series) to meet these changes in the bearing environment. They have been accepted in their main application area of machining centers.

The word ROBUST was chosen to appropriately describe their ability to be “insensitive to changes in the bearing environment” but ROBUST bearings also have low heat generation characteristics. Because of this, ROBUST bearings can not only perform well in machining centers but the same design philosophy can be used to meet the requirement for the higher speeds needed by thrust angular contact ball bearings in lathes. Formerly, lathe spindles were operated at 500 000~600 000 $d_m n$, but recently some precision lathes require a spindle speed of nearly 1 000 000 $d_m n$. ROBUST thrust angular contact ball bearings (designated BAR) developed to meet the new requirement can achieve a 20% faster speed performance while maintaining other performance requirements (rigidity, grease life). On the other hand, the change to the integral motor type has increased the length of the spindle. As a result, the axial thermal expansion has increased and the need to allow for expansion of the spindle has come to have greater importance. Generally, the elongation of the spindle is absorbed by axial movement in either of the following ways:

(1) the outer ring of an angular contact ball bearing sliding in the housing; or
(2) the inner ring and its roller set moving axially within the outer ring of a cylindrical roller bearing.

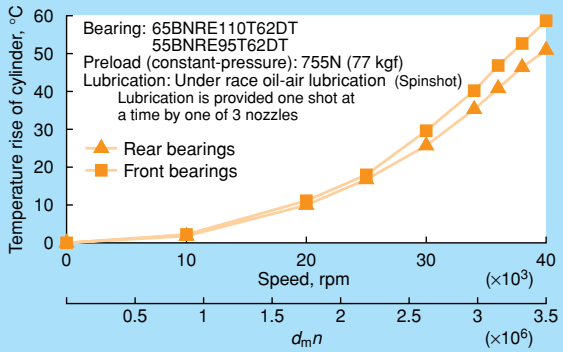

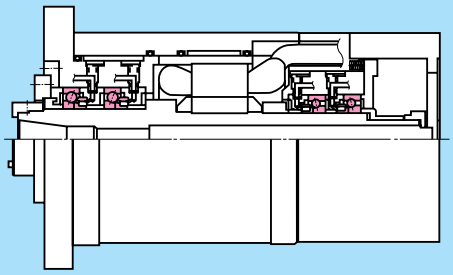

Testing machine structure

Fig.1 Temperature rise with oil-air lubrication and constant-pressure preload

Fig. 1 shows the construction and characteristics of an actual spindle on which a ROBUST angular contact ball bearing is used for the first option.

On conventional belt driven spindles, double row cylindrical roller bearings were most often used to take the belt tension at their rear (free) end. In the days when spindle speeds were about to reach or exceed a level of 1 500 000 $d_m n$, there was recognition that cylindrical roller bearings were not suited for, and not easy to apply to, such high-speed operations because of lubrication difficulties and other unstable factors. The subsequent development of spindles containing a built-in motor, on whose rear end a single row cylindrical roller bearing can be used, promised the advantage of simplifying the slide mechanism. Bearings able to run at higher $d_m n$ values needed to be developed.

3. Concept of the Development

To meet these needs, NSK started development of super-high speed cylindrical roller bearings. Given the variation of spindle arrangements, two types of cylindrical roller bearings are generally used on machine tools. One is N type; single row cylindrical roller bearings whose outer rings have a straight cylindrical form and whose inner rings have ribs. The other is NN type; double row cylindrical roller bearings.

To achieve high-speed performance, the following problems had to be solved:

(1) Abrasion and seizure of roller ends and ribs
(2) Cage design with higher strength
(3) Establishment of optimum lubrication method

The following subsections describe some of these problems and how they were overcome.

3.1 Abrasion and seizure of roller ends and ribs

In a cylindrical roller bearing, each roller can skew because of the clearances between the roller ends and the ribs (Fig. 2.).

If, in applications where the inner ring of the bearing is rotated, the rollers begin to skew, a gyroscopic moment acts to accelerate this skewing. If the bearing is running at high speed, this moment can be high enough not to be neglected (Equation (1)). Consequently, the rollers are forced to rotate and revolve in a skew state while being pressed against the ribs (Fig. 3).

$$S = I_x \cdot \omega_c \cdot \omega_B \cdot \sin\theta - (I_x - I_z)\,\omega_c^2 \cdot \sin\theta \cdot \cos\theta \quad \ldots\ldots\ldots (1)$$

S : gyroscopic moment
I_x: moment of inertia around axis of rotation of roller
I_z: moment of inertia around axis orthogonal to I_x
ω_c: revolution of roller around axis of inner ring
ω_B: rotation of roller around its own axis

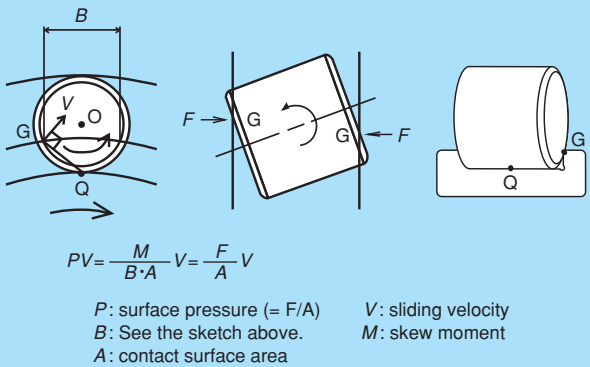

Fig. 2 Conditions of skewed roller

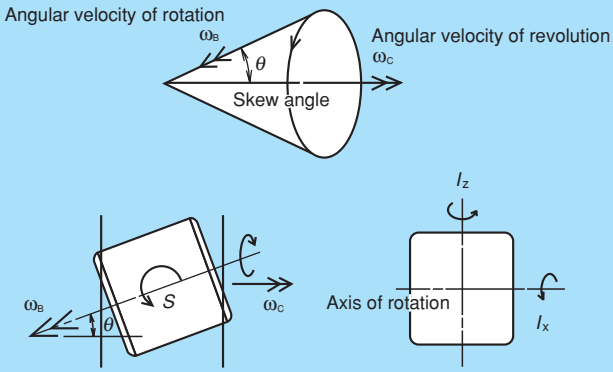

Fig. 3 Gyroscopic moment (S) and inertia moment acting on rollers (In applications with inner ring rotation)

Minute geometrical inaccuracies cause each roller to have a small fluctuation skewing moment as they rotate. Moreover, when negative radial clearance (pre-load) becomes larger, the roller skewing can cause additional axial forces giving higher *PV* values (*P*=surface pressure, *V*= relative sliding velocity) between the roller ends and the ribs. Considering these factors, we selected four areas for design improvement.

(1) An optimum design of the ribs and the clearances between the ribs and roller ends such that a fluid lubricant film may be formed on the contacts between them.
(2) Minimization of *PV* value at the contact between the roller ends and the ribs.
(3) A design arrangement to keep the gyroscopic moment above the fluctuating skew moment, such that the rollers may smoothly revolve around the bearing axis while maintaining a constant skew angle and constant contact with the ribs, without wobbling.
(4) Edge improvements—the design of the chamfered edges of the roller ends and the chamfered edges of the ribs.

3.2 Cage design

The cage is designed for high-speed running. Although usually running at a speed of only 40 to 45% of the inner ring, it is subject to constant heating caused by the complicated collision and local sliding of rollers (at roller and pocket contacts and guide surfaces). Thus, the cage is at risk of fracture, seizure and wear and may be regarded as a significant factor in attaining higher speeds.

The cage material can be metal if jet lubrication is applied. For applications such as machine tools where there may be a very low lubrication rate (to prevent churning), the wear on metal cages makes them unsuitable. Promising candidates are engineering polymers, tough, light and resistant to heat and wear.

For cage design, it is very important to select a suitable material and establish specifications to minimize self-induced oscillations due to friction between the rollers and the pocket and guide surfaces.

3.3 Approach to low heat generation

It is important to give due consideration to the prevention of rib seizure; this is not easy and suitable lubrication can be difficult. From the viewpoint of low heat generation, it is also important to minimize the wear of the roller and raceway contact surfaces by means of:

(1) A decrease in the roller and raceway contact surface area by shortening the straight length of the rolling contact surface and also by enlarging the crowning of the rollers.
(2) An increase in the number of rollers.
(3) Using rollers whose length is reduced but not by an amount that significantly affects rigidity. This can also reduce the heating of the ribs and is therefore very effective.

For (3) above, its effect on lowering temperature rise was actually verified in tests. Fig. 4 shows the results.

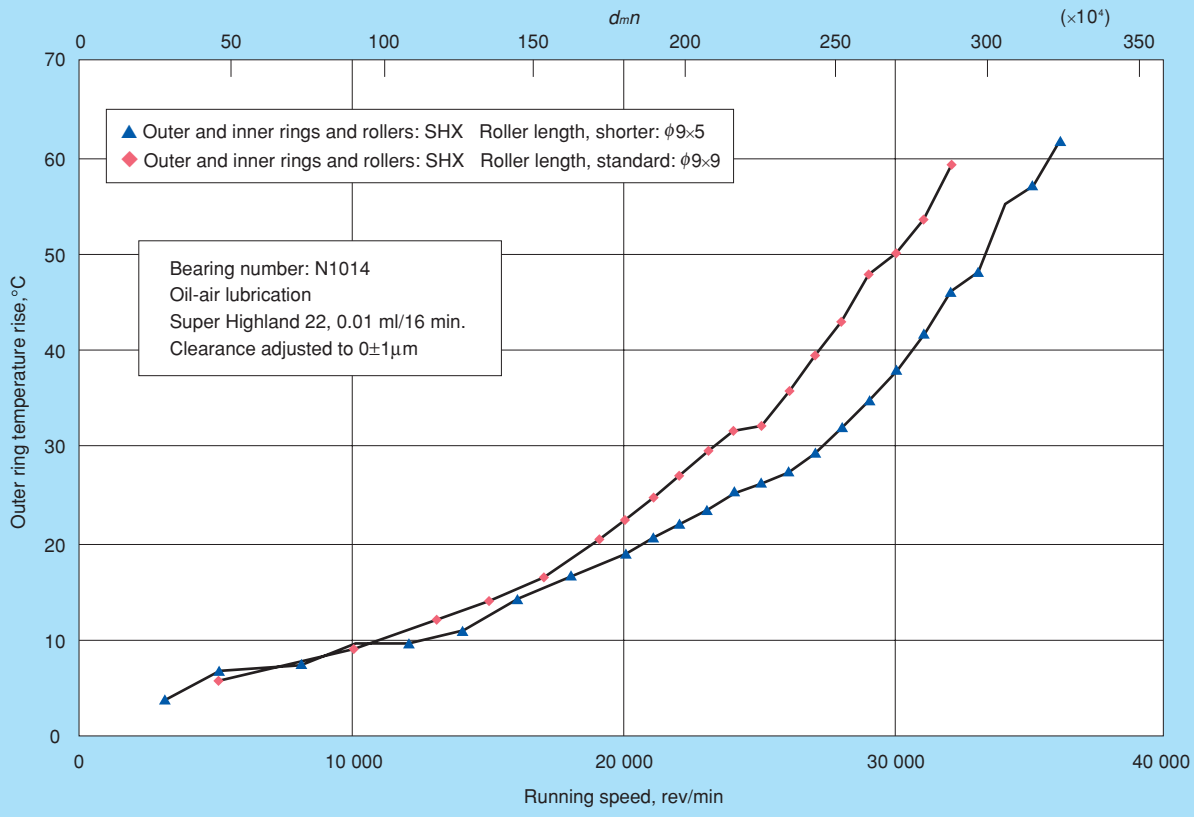

Fig. 4 High-speed cylindrical roller bearing test results

4. Design of ROBUST Cylindrical Roller Bearings

4.1 Bearing specification

To increase the resistance of the ribs to seizure, described in 3.1 above, we made the following changes:

(1) optimization of rib height

(2) control of clearance between rollers and ribs

(3) improvement of roller accuracy

Also, to ensure low heat generation, we reduced the roller length to an extent not affecting its function (as mentioned in 3.3 above). As a result, the range design features rollers smaller in size and smaller in number than those of standard NSK cylindrical roller bearings.

4.2 Bearing material

The inner and outer rings and the rollers are made of surface-hardened SHX, a unique material developed by NSK. SHX is a heat-resistant steel having excellent resistance to seizure and wear properties and an excellent life (3 to 4 times longer than that of SUJ2). ROBUST series bearings produced with SHX have already been used in many high-speed spindles and proved their performance.

In super high-speed operations, inner rings are generally known to have a tendency to be forced into a fracture mode by high hoop stresses. With SHX, an inner ring has a remarkable freedom from such fractures because its internal residual stress can counter the hoop stresses.

Ceramics would be a good choice of material for the rollers as they have low heat generation characteristics but they do have cost problems.

4.3 Cage

The cage design includes outer ring guidance and a cage material of PEEK (polyether etherketone). The polymer is reinforced with fiberglass and has excellent attributes of lightness of weight, and resistance to heat, wear, and fracture. Its ability to be manufactured by cost effective injection molding is an additional good feature. The pocket design also takes into consideration the material's strength, low deformation and good frictional characteristics for high speed use.

5. Performance Evaluation

Fig. 5 shows the test results for these cylindrical roller bearings.

The test bearing was an N1014 single row cylindrical roller bearing having an inside diameter of 70 mm, an outside diameter of 110 mm and a width of 20 mm. It comprised inner and outer rings and rollers in SHX. Also tested for comparison were two other configurations: a similar bearing but with ceramic rollers and a similar bearing but where the cage was of a standard roller guide type and made of reinforced nylon. The cylindrical roller

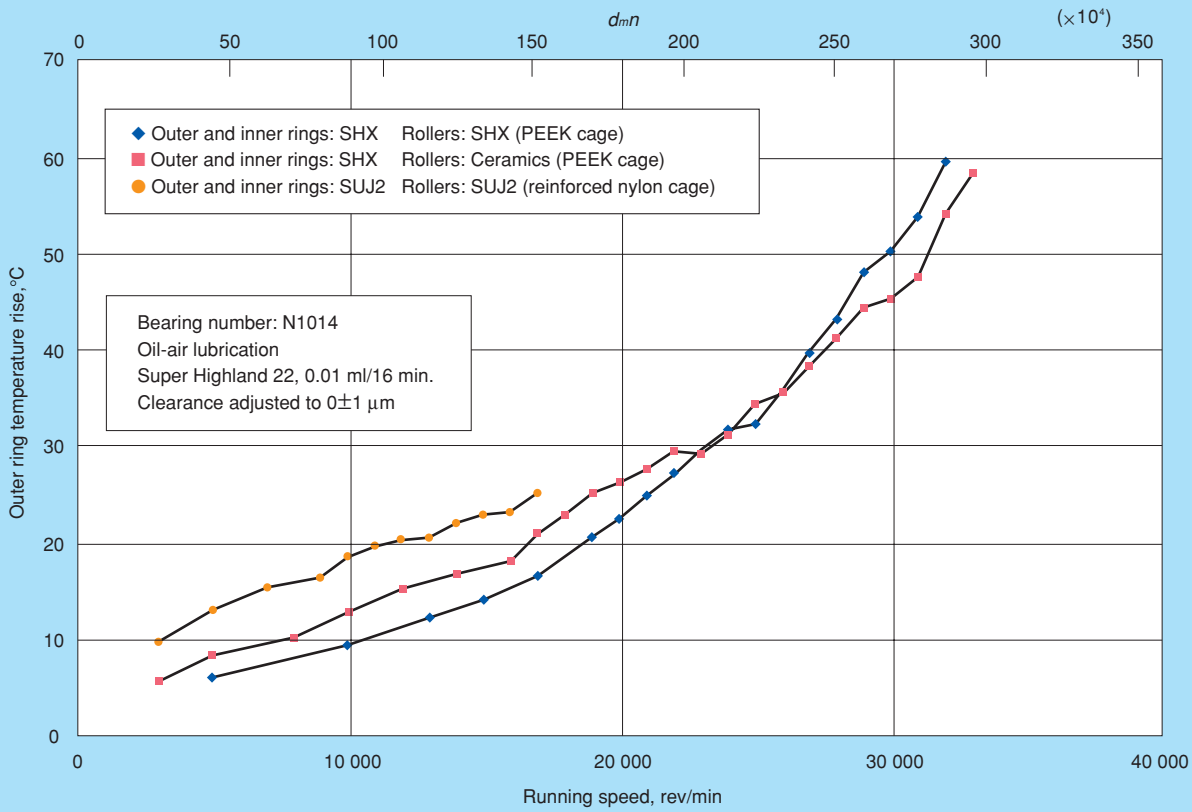

Fig. 5 High-speed cylindrical roller bearing test results

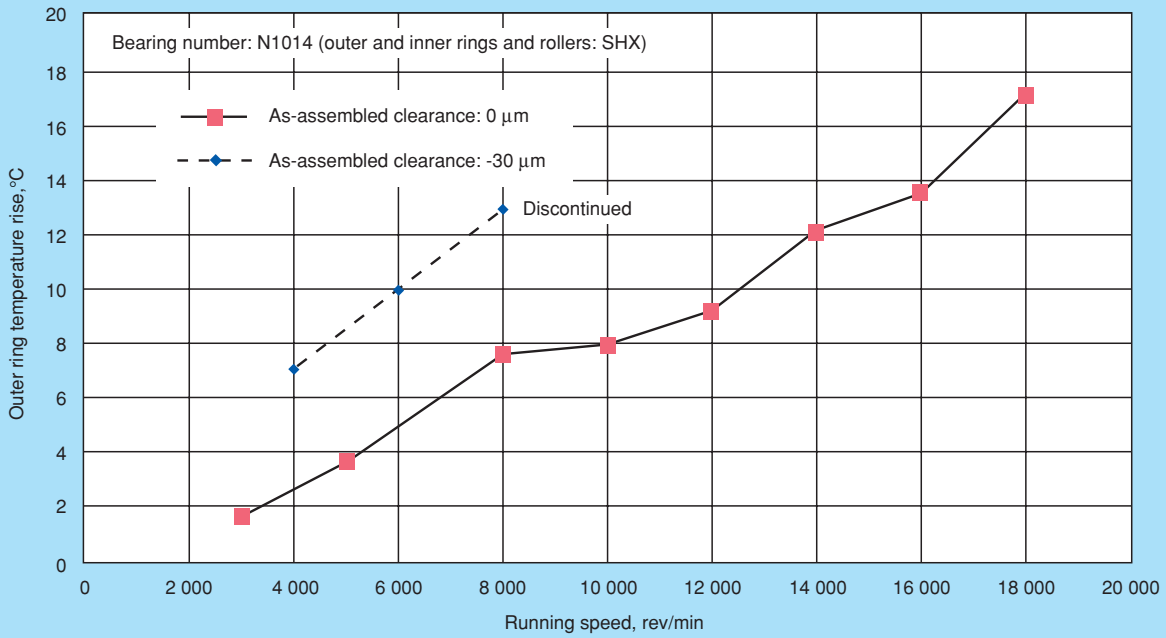

Fig. 6 Rotation test results—grease lubrication

bearings had been assembled to have no radial clearance and were oil lubricated.

As the test results indicate, the test bearing developed to embody the design improvements could run up to 3 000 000 $d_m n$. Its temperature rise, when compared with that of the bearing having ceramic rollers, did not show any significant difference up to 2 500 000 $d_m n$. With temperature rise characteristics of bearings considered, this bearing can operate in practical situations at up to 2 000 000 $d_m n$. When cost efficiency is taken into account, therefore, the all-SHX bearing is very promising for commercial applications.

6. Practical Application of High-Speed Cylindrical Roller Bearings

6.1 Assembly arrangements

For use in machine tools, duplex angular contact ball bearings are set with preload to eliminate spindle radial movement.

For cylindrical roller bearings, a negative radial clearance (pre-load) is also often required for the purpose of eliminating roller drop sound or cage noise during low-speed operation. For this reason, the tested bearings as described above had no initial radial clearance.

However, the spindle continues heating as it continues running causing a temperature difference between the inner and outer rings. As a consequence, the radial clearance is decreased and the internal stress of the bearing is increased, potentially shortening bearing life.

Fig. 6 shows the results of a running speed limit confirmation test of bearings assembled to have an initial radial clearance of -30 µm. To ensure minimal lubrication, the bearings were tested under grease lubrication.

It is known from the previous test work that restricting the spindle temperature rise can increase bearing life. Thus, minimizing inner and outer ring temperature differences as well as the lubrication can be most beneficial. In fact, spindle cooling is actually used to stabilize bearing performance. Some advanced machine tools really have exemplary spindle cooling arrangements whose effectiveness has been verified.

6.2 Lubrication

In an oil-air lubrication system, a very small amount of oil is applied at fixed intervals. There is a known phenomenon of irregular heat generation from the bearing caused by uneven oil application. Fig. 7 shows an example of actual bearing outer ring surface temperature measurements. As a means to prevent the fluctuating heat generation from the bearings, a unit has been developed capable of applying a smaller quantity of oil at controlled

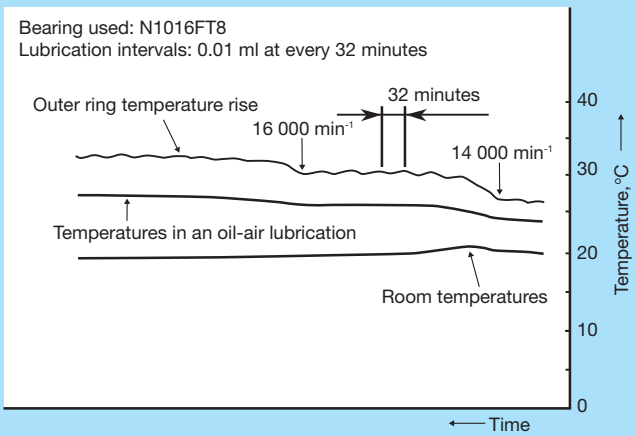

Fig. 7 An example of actual bearing outer ring surface temperature measurements

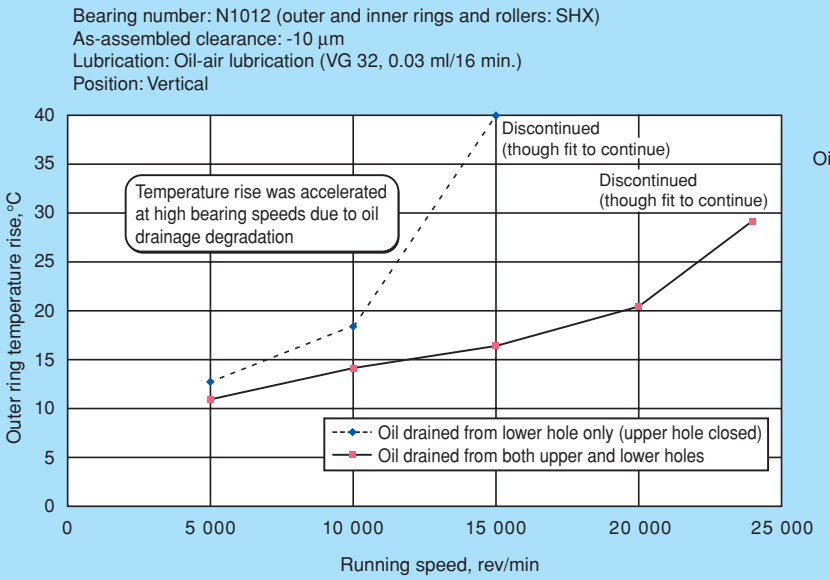

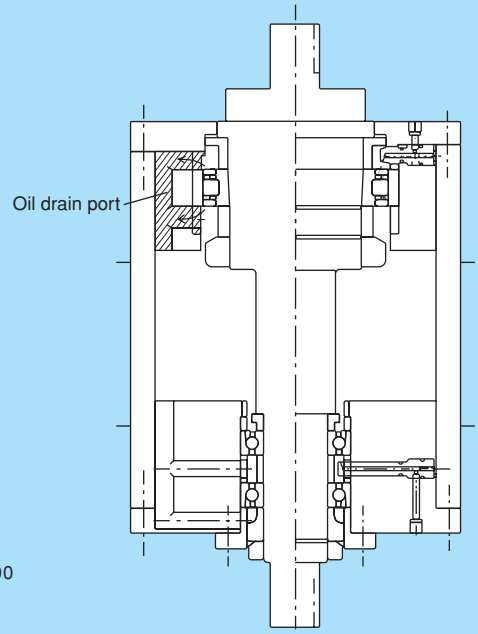

Fig. 8 Rotation test results - effect of oil drain hole

intervals. This innovative unit, capable of applying 0.001 ml of oil at intervals of one minute has been developed and marketed. By comparison, the dispensed amount of a conventional unit is 10 times higher at 0.01 ml—but at longer intervals of 8 to 16 minutes. At NSK, we have checked the performance of the new unit and verified the effectiveness of averaging the oil dispense rate for reducing the thermal cycling. It is to be noted that dispensing the oil in such small quantities as 0.001 ml volumes tends to cause it to be converted into oil mist. We have verified this with experiments revealing different lubrication environments.

As well as lubrication control, it is known that an important aspect of spindle design is the smooth oil drainage. Fig. 8 shows the results of our verification test in this respect.

Oil mist lubrication is often used in bearings for medium-speed spindles due to the simplified design of the lubrication system. However, it is important to ensure that the supply quantity is accurate. One of the typical problems encountered is uneven distribution owing to the branching of supply piping. Another common problem relates to the low air flow-rate used to generate the mist, often as low as one tenth of the flow-rate for oil-air systems. As a consequence, if the bearing is operated beyond certain speeds, the oil mist flow cannot pass through the air curtain formed by the rotation of the bearing.

7. Future Targets

In addition to the angular contact ball bearings already forming the ROBUST series, we have completed the development of ROBUST series cylindrical roller bearings. They are expected to help support the development of higher-speed spindles containing integral motors.

Our next step is the development of a range of grease-lubricated, highly reliable, cost-effective bearings, responding to environmental and economic requirements in the 21st century. Based on a holistic approach to spindle design, NSK is taking steps to develop a systematic design philosophy for spindle bearings and their associated parts. When the needs of bearing users and the proposals from bearing manufacturers converge an outstanding solution will emerge.

Yasushi Morita

Yukio Ohura

Ultra Lightweight, Low-Cost TRZ Clutch Release Bearing

1. Foreword

Recently due to global environmental problems, automotive design is such that vehicles are required to be sensitive to the environment and economical in fuel consumption. In responding to such market needs we developed and, in 1999, introduced to the marketplace the TKZ type clutch release bearing. Weight and cost were reduced whilst maintaining the long life and high quality of the preceding clutch release bearing.

The ultra lightweight, low-cost TRZ clutch release bearing (Photo 1) we have now developed is a self-centering type with a plastic sleeve where weight and cost are greatly reduced even from the TKZ type. We describe this advancement here.

Photo 1 TRZ clutch release bearing

2. Design

The design of the TRZ clutch release bearing is shown in Fig. 1.

The TRZ clutch release bearing adopted the simplest mechanism of two clinch springs inherited from the TKZ type and the bearing has a further design optimization.

The T-type plastic sleeve is integrated with the anvil function. This results in simplifying the assembly. It now comprises only the bearing, the plastic sleeve and two clinch springs.

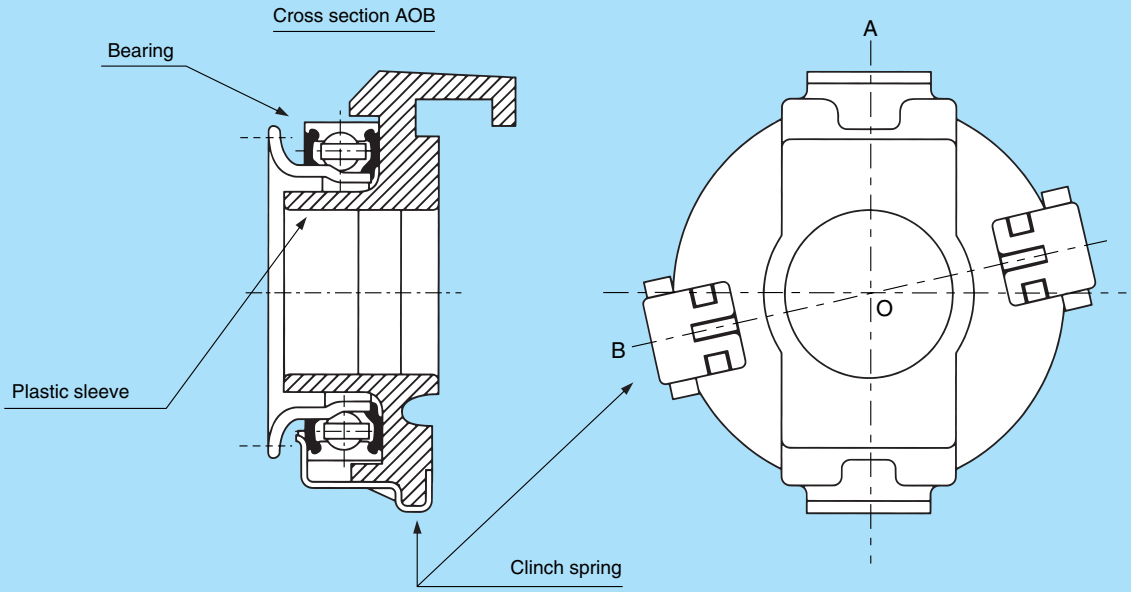

Fig. 1 TRZ clutch release bearing

3. Features

(1) The steel plate anvil is eliminated.
Its function, receiving the input load from the fork, is integrated into the plastic sleeve. This provides further weight and cost reductions to the unit.

(2) Many of the newest long-life promoting technologies of NSK like the ENC grease, materials and seals adopted by the TKZ type clutch release bearing, are used here. The TKZ extended life is thus perpetuated in the new TRZ design.

Table 1 Results of a one-million-cycle endurance test

	Before test	After test	Results
Sound pressure, dB	50	58	OK
Centering resistance, N	77	48	OK
Worn amount of anvil formed plastic, mm	—	0.31	OK
Worn amount of top end of fork, mm	—	0.05	OK

4. Performance

The TRZ bearing cleared the evaluation criteria of one million release cycles in the clutch release endurance test. The test result is shown in Table 1. The results show that the TRZ clutch release bearing design can be brought into the marketplace.

5. Conclusion

The TRZ clutch release bearing is a compact and lightweight bearing that not only meets current requirement demands, but also meets anticipated requirements well into the future.

This clutch release bearing also has the potential of furthering cost reductions.

We anticipate and look forward to marketing of this product on a global scale.

Low-Torque Bearing for Fan Motors and Vacuum Cleaner Motors

Recently, household electrical appliance manufacturers have been driven to significantly improve the operating efficiency of their products. Consequently, NSK has developed a low-torque ball bearing for use in vacuum cleaner motors and air conditioner fan motors. An overview of this development is presented herein.

1. Bearing Design

Fig. 1 shows the construction of the standard ball bearing and that of the low-torque bearing. The bore, outside diameter and width dimensions are the same for both (Bearing No.: 608), but by modifying internal features (P.C.D., ball diameter, etc.) reduced friction torque was attained. A comparison of basic bearing specifications is listed in Table 1.

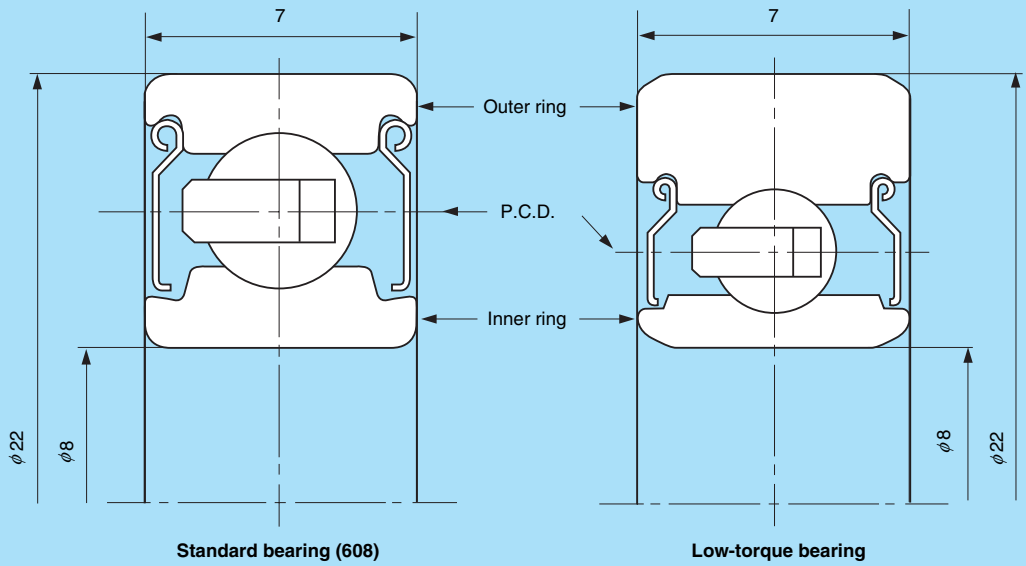

Fig. 1 Construction of low-torque bearing

Table 1 Specification

Item \ Bearing No.	608 (Standard)	Low-torque bearing
Outside diameter, mm	22	22
Bore, mm	8	8
Width, mm	7	7
Number of balls	7	7
Cage	Plastic cage	Plastic cage
Shield	Steel plate	Steel plate
Grease	NS7, NSC, etc.	NS7, NSC, etc.
Allowable axial load, N	730	1 100
Basic static load rating, N	1 370	910
Basic dynamic load rating, N	3 300	2 240

*The basic load rating of the low-torque bearing is lower than the standard one, but in the actual applications endurance is mainly determined by grease life and the requirement for a light load can be satisfied.

2. Features

(1) Compared with the current bearing the dynamic friction torque was reduced by 40 to 50%. (Figs. 2 and 3) Particularly at high speed, excellent torque reduction was confirmed. (Fig. 4)

(2) Since the boundary dimensions of the low-torque bearing are the same as those of the standard bearing, changing from a standard design to the low-torque bearing is simple.

(3) By processing the inner/outer ring and balls for high precision, and utilizing lithium soap grease developed by NSK, the low-torque bearing is quieter than the standard design.

3. Applications

This new bearing can be used for motors of many domains requiring high performance, for example:

- Vacuum cleaner motor
- Fan motor for air conditioner
- Motor for air cleaner
- Cooling fan motor

4. Conclusion

We assume that the requirement for higher performance motors for household appliances will become keen. We will continue development to build a series of such low-torque bearings.

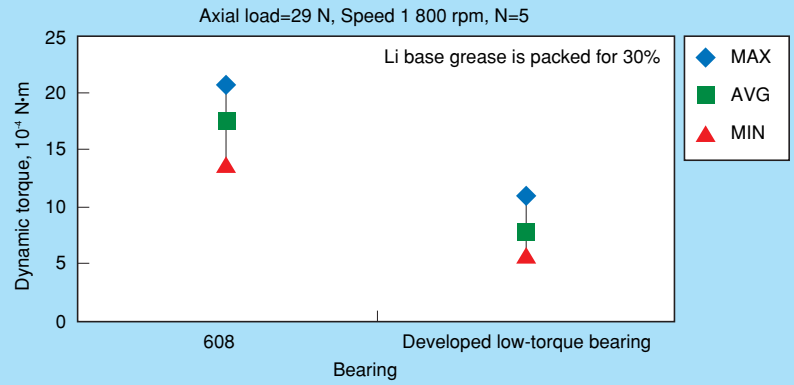

Fig. 2 Comparison of running torque at 1 800 rpm

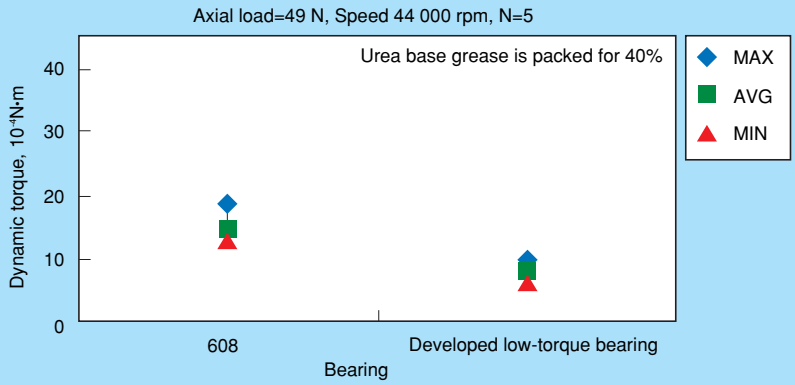

Fig. 3 Comparison of running torque at 44 000 rpm

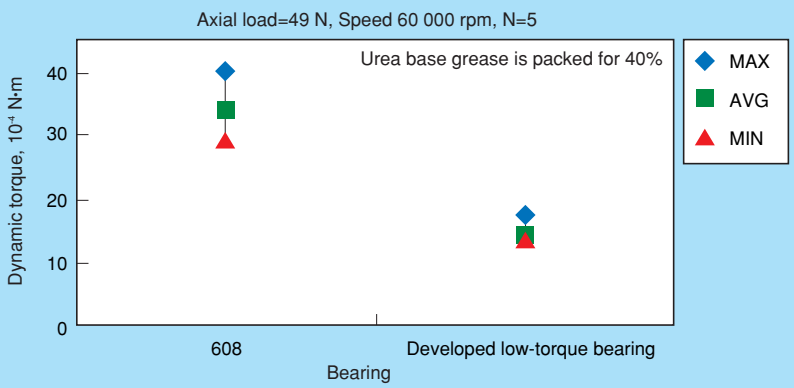

Fig. 4 Comparison of running torque at 60 000 rpm

Bearings for Corrosive Environments

Semiconductor and LCD panel manufacturing, food processing, photographic production processes, etc., often result in bearings being exposed to water, alkalis, acids or corrosive vapors. In such environments, bearings made of the usual high carbon chromium steels rust quickly and their use is restricted. NSK new technologies can be used to produce bearings suitable for such arduous duties. Highly corrosion resistant stainless steel, anticorrosive coatings and ceramics all play their part (Photo 1).

This article reviews designs for corrosive environments and some application examples.

1. Specifications, Features and Application Examples

1.1 Hybrid bearings for aqueous environments

The bearings used in equipment for food processing, bottle cleaning, etc., are exposed to water splash or even immersion. We show in Fig. 1 an example of bearings for corrosive environments (hybrid bearings with ceramic balls) used in food-processing machinery. The standard specifications of bearings for aqueous exposure are inner and outer rings made of martensitic stainless steel and ceramic balls. The endurance life in water of these bearings is shown in Fig. 2. The hybrid bearings have a life about 10 times longer than stainless steel bearings, as has been shown in many applications.

1.2 Bearings for use with alkalis and weak acids (Anti-corrosion coated bearings, oxide-type ceramic bearings)

Bearings used in semiconductor and LCD panel production equipment and in cleaning processes for hard disk production are subjected to highly corrosive alkalis and acids or their vapors. We show in Fig. 3 an example of bearings for semiconductor production equipment. In this instance, a polishing process. The bearings must be resistant to corrosion to exhibit the required endurance in this harsh environment. The bearings have inner and outer rings and balls made from stainless steel coated with an anti-corrosion treatment. Alternatively, bearings may be constructed with ceramic inner and outer rings and balls and featuring a fluorine polymer cage. The endurance life of these ceramic bearings in water is shown in Fig. 4. The oxide-type ceramic chosen gives a bearing with longer life and lower cost than bearings using other ceramics.

1.3 Bearings for strongly acidic environments (carbide-type ceramic bearings)

The bearings used in the etching devices, cleaning equipment, etc., come into contact with strongly acidic corrosive solutions or vapors. Fig. 5 shows a bearing suitable for the corrosive environment in special cleaning equipment. An application involving such a highly corrosive environment benefits from carbide-type ceramic components which are not corroded, even by strong acid; similarly, fluorine polymer cages show appropriate resistance. The endurance life of anti-corrosion ceramic bearings is shown in Fig. 6. Compared with bearings of other ceramics, carbide-type ceramic bearings have much longer life together with stable torque characteristics.

2. Conclusion

Bearings that exhibit good endurance in a range of highly corrosive environments are possible through the use of materials such as stainless steel together with anticorrosive coatings and the use of specific types of ceramics.

Ball screws and linear guides using these same new technologies are also available.

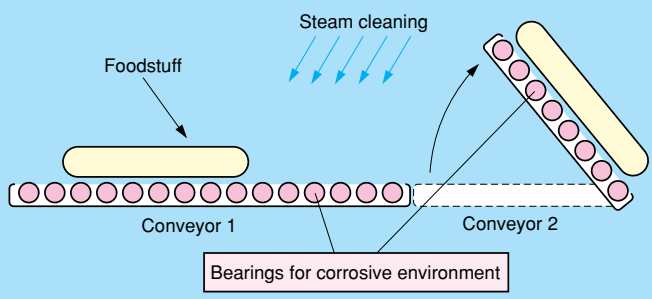

Fig. 1 Food processing machinery

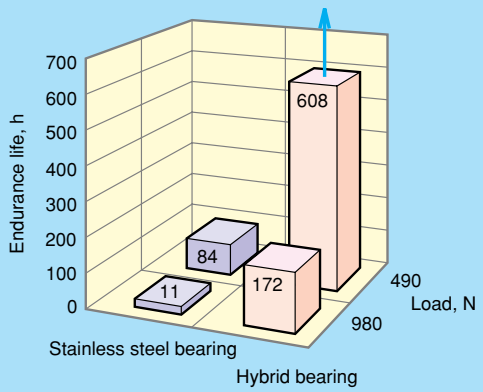

Fig. 2 Endurance life of hybrid bearings in water

Photo 1 Bearing for corrosive environments (Ceramic bearings)

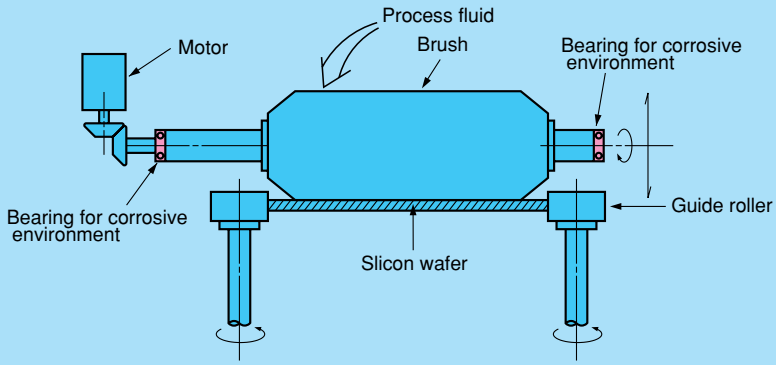

Fig. 3 Semiconductor production device (polishing process)

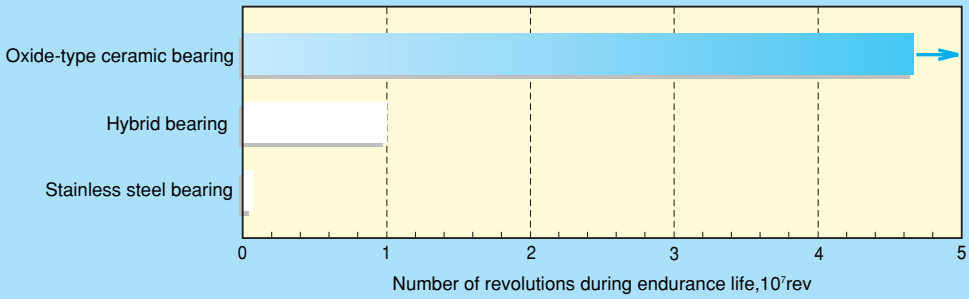

Fig. 4 Endurance life of ceramic bearings in water

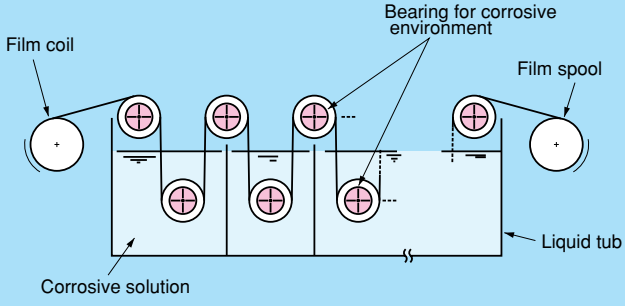

Fig. 5 Cleaning device

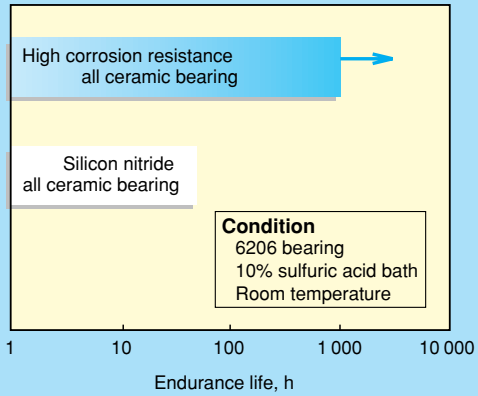

Fig. 6 Endurance life of highly corrosion-resistant ceramic bearing

Aqua-Bearing™—Special Fluorine Plastic Rolling Bearing for Highly Corrosive Environments

Bearings used in equipment for the manufacture and processing of many products are required to work in corrosive environments. LCDs, hard disks, semiconductors, food processing, pharmaceuticals and specialized cleaning operations are typical applications where bearings are exposed to chemicals (water, acid, alkali) by either splash or vapor presence.

NSK has developed a special fluorine plastic rolling bearing, Aqua-Bearing™, as a highly corrosion resistant, low cost, light load bearing to respond to these demanding industrial applications.

In this article we describe the bearing and its features.

1. Design and Specification

The appearance and design of Aqua-Bearing™ are shown in Fig. 1 with its standard specification in Table 1.

The standard bearing range is listed in Table 2. We can also address demands outside of this range.

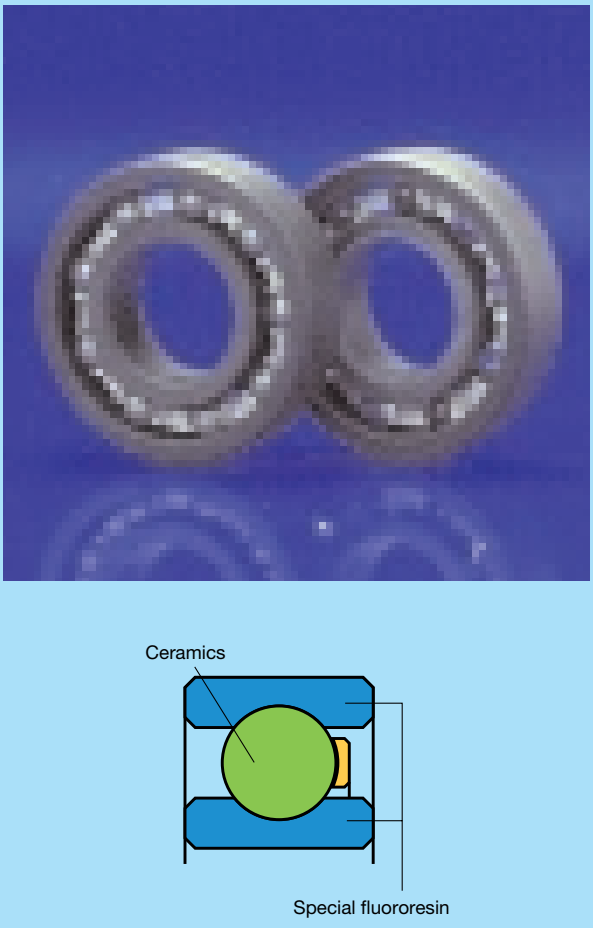

Fig. 1 Appearance and structure of Aqua-Bearing™

2. Features

(1) Excellent corrosion resistance

By using a special fluorine plastic for the inner and outer rings and a fluorine plastic cage, we have achieved a corrosion resistance equal to ceramic bearings and better than that of previous plastic rolling bearings made of PE (polyethylene) or PPS (polyphenylene sulfide). Aqua-Bearing™ is able to handle applications even in strong acids or alkalis, ozonized water, various kinds of vapor and halogen gases (Table 3).

(2) Excellent endurance life

By using fiber reinforced fluorine plastic for the inner and outer rings, the Aqua-Bearing™ has an endurance life of over 1 000 times that of a stainless steel bearing (AISI440C) and 5 times that of previous PE bearings under a light load in an acid solution (Figs. 2 and 3).

(3) By fiber reinforcement, strength and rigidity have been increased.

(4) Operation temperature range: up to ~150°C

Table 1 Standard specification

Inner/outer ring	Special fluorine plastic
Rolling element	Ceramics (or special high-strength glass)
Cage	Fluorine plastic

Table 2 Standard bearing No.

Shaft diameter	Bearing No.	Boundary dimension, mm		
		Bore	Outside diameter	Width
10	6900PLCSN14T36	10	22	6
	6000PLCSN14T36	10	26	8
12	6901PLCSN14T36	12	24	6
	6001PLCSN14T36	12	28	8
15	6902PLCSN14T36	15	28	7
	6002PLCSN14T36	15	32	9
17	6903PLCSN14T36	17	30	7
	6003PLCSN14T36	17	35	10
20	6904PLCSN14T36	20	37	9
	6004PLCSN14T36	20	42	12
25	6905PLCSN14T36	25	42	9
	6005PLCSN14T36	25	47	12

Structure of bearing No.: □□□□ PLCSN14T36
✻ Other bearing designations are also available.

3. Application Example

Aqua-Bearing™ can be used in water, chemicals (acids, alkalis), exposed to splash or vapor of various chemicals or even running in a dry environment.

Application examples include the following industry sectors:

(1) LCD, hard disk and semiconductor manufacturing
(2) Food processing
(3) Pharmaceuticals
(4) Chemicals
(5) Surface treatments

4. Conclusion

The Aqua-Bearing™, featuring a special fluorine plastic construction, which we have presented here, can satisfy customer needs as a rolling bearing exhibiting excellent corrosion resistance and endurance life under such diverse and highly corrosive environments related to LCD panels, hard disk and semiconductor equipment, food processing and pharmaceutical machinery.

Subsequently, we are developing new products to satisfy a marketplace with increasingly sophisticated needs.

Table 3 Corrosion resistance

	Aqua-Bearing™ Special fluorine plastic rolling bearing	PE	PPS	Ceramics
Concentrated sulfuric acid	○	△	△	○
Hydrochloric acid	○	○	○	○
Hydrofluoric acid	○	○	×	○
Aqua regia	○	△	×	○
Hydrogen peroxide	○	○	○	○
Ozonized water	○	×	○	○
15% acetic acid	○	△	△	○
75% nitric acid	○	×	×	○
40% chromic acid	○	×	△	○
Halogen gas	○	×	○	○

Corrosion resistance evaluation
○ ... Not corroded
△ ... Partially corroded
× ... Corroded

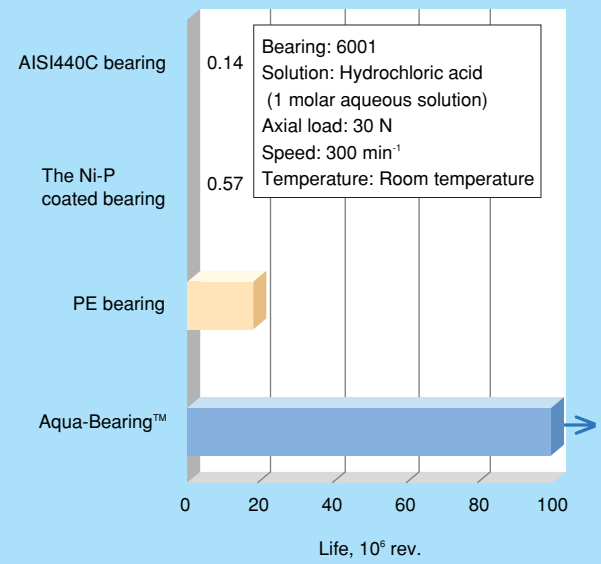

Fig. 2 Life in hydrochloric acid

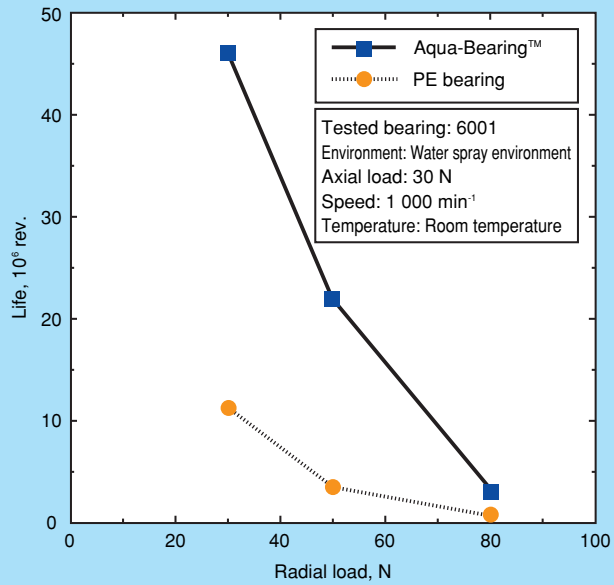

Fig. 3 Relationship of load with life (Water spray environment)

High Performance Seals for Ball Screws

Processing machines such as laser cutting machines use numerous dust-proofing measures to protect the drive system from dust particles, spatter and other contaminants. Often times, these measures are omitted due to size and cost restrictions resulting in the ball screws being exposed to severe contamination. The conventional labyrinth seals for ball screws are limited in their capacity to protect against dust and other such contaminants. As a result, there is an increasing demand for improved dust-proof seals. NSK has been developing a high performance seal, which has improved protection against dust and other such contaminants.

This article presents a high performance seal, which NSK has developed for better dust protection and longer life in contaminated environments.

1. Structure

The high performance seal is compact in design due to its lip shape resembling the cross section of the screw shaft. This seal is also designed for low torque to prevent excessive temperature rise. Fig. 1 shows an example of the high performance seal. In addition, the ball grooves of the screw shaft are designed to improve seal performance and reduce the entry of foreign particles into the nut.

The NSK K1™ lubrication unit is installed as standard on these units, in order to further protect the ball screw from contamination as well as to improve life. The addition of the NSK K1™ unit leads to a longer ball nut than the nut with standard seals.

Photo 1 shows a ball screw equipped with a high dust-proof performance seal.

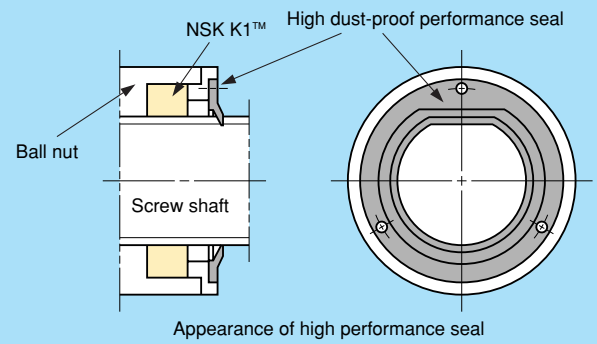

Fig. 1 Appearance of high performance seal

2. Features

(1) High dust-proof performance

To evaluate the performance of the seals, we measured the contamination volume of foreign particles that penetrated the seals through application of a mixture of grease with steel particles of less than 30 μm diameter. This mixture was applied to the screw shaft and the nut stroked over the area.

Fig. 2 shows the results of this test. We measured the volume of contamination that penetrated through the seals after the nut had been stroked over the shaft. The high performance seal reduced contamination volume to less than 1/15 of the standard seal.

Photo 2 shows the appearance of the test piece before and after the passage of the high performance seal.

(2) Long Life

To evaluate the life of the ball screw under a severe contamination environment, we conducted the endurance tests of the ball screw while applying a mixture of steel particles and a small amount of grease at fixed intervals.

The test results are shown in Fig. 3. The life of the ball screw with the high performance seals was over 4 times the life of a ball screw with standard seals.

3. Availability

The high performance seal is an option available on custom-made ball screws. The development of the seals for several screw diameters between 25 and 50 mm has been completed. The development on other sizes will be considered upon request.

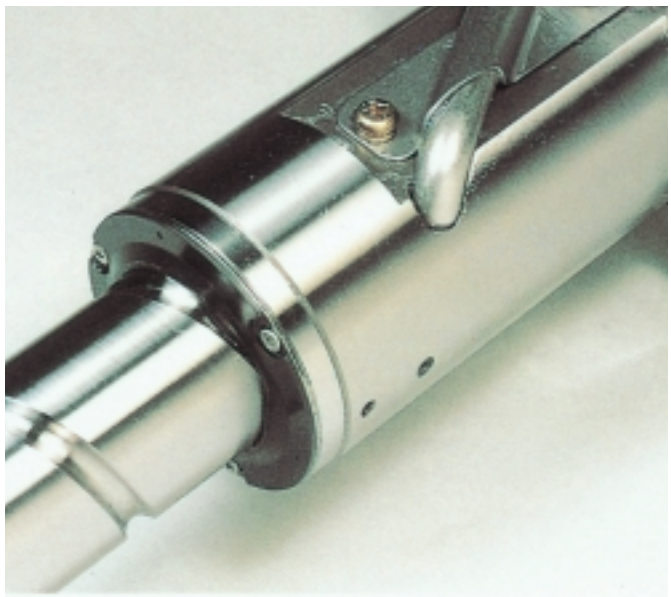

Photo 1 Ball screw equipped with high performance seal

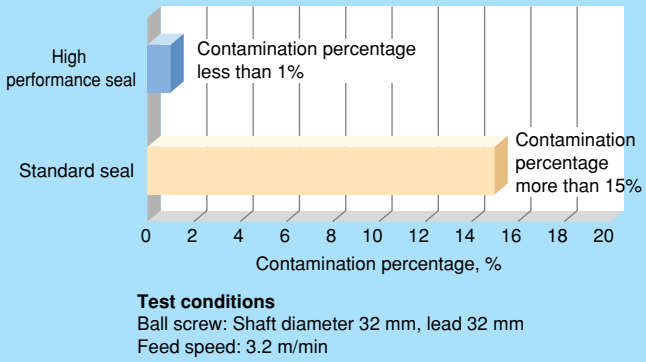

Test conditions
Ball screw: Shaft diameter 32 mm, lead 32 mm
Feed speed: 3.2 m/min

Fig. 2 Comparison of contamination volume

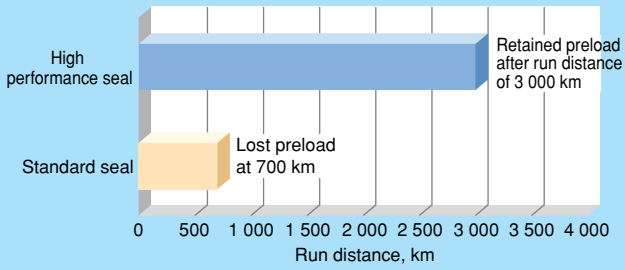

Test conditions
Ball screw: Shaft diameter 32 mm, lead 32 mm
Feed speed: 40 m/min
Stroke: 700 mm
Load: 1.4 kN
Lubrication: Grease (only initial packing)

Fig. 3 Endurance test under exposure to steel particles

Before passage

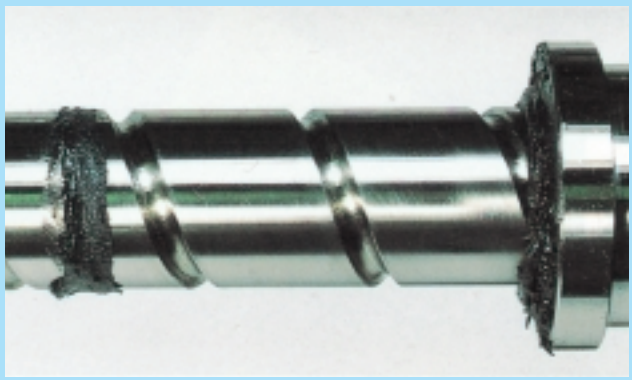

After passage

Photo 2 Appearance before and after passage of high performance seal

4. Application

High performance seals are efficient for use in applications where foreign particles pose a contamination problem, such as laser cutting machines, woodworking machines, etc.

5. Conclusion

It is assumed that the environments that ball screws are used in will become more and more severe. As a result it is anticipated that the demand for the high performance seals and the NSK K1™ lubrication units will also increase.

Notes:

Notes:

Notes:

Worldwide Sales Offices and Manufacturing Plants

NSK LTD.–HEADQUARTERS, TOKYO, JAPAN www.nsk.com
AMERICAS & EUROPE DEPARTMENT: Nissei Bldg., 6-3, Ohsaki 1-chome, Shinagawa-ku, Tokyo 141-8560, Japan
P: 03-3779-7120 F: 03-3779-7433 T: 2224280 NSK BRG J C: 81
ASIA MARKETING & SALES DEPARTMENT: Nissei Bldg., 6-3, Ohsaki 1-chome, Shinagawa-ku, Tokyo 141-8560, Japan
P: 03-3779-7121 F: 03-3779-7433 T: 2224280 NSK BRG J C: 81

Africa

South Africa:

NSK SOUTH AFRICA (PTY) LTD.
JOHANNESBURG 25 Galaxy Avenue, Linbro Business Park, Sandton, 2146, Gauteng, South Africa
P: (011) 458 3600 F: (011) 458 3608 C: 27

Asia and Oceania

Australia:

NSK AUSTRALIA PTY. LTD.
MELBOURNE 11 Dalmore Drive, Scoresby, Victoria 3179, Australia
P: (03) 9764-8302 F: (03) 9764-8304 C: 61
SYDNEY Unit 1, Riverside Centre, 24-28 River Road West, Parramatta, N.S.W. 2150, Australia
P: 02-9893-8322 F: 02-9893-8406 C: 61
BRISBANE 91 Wellington Road, East Brisbane, Queensland 4169, Australia
P: 07-3393-1388 F: 07-3393-1236 C: 61
ADELAIDE 64 Greenhill Road, Wayville, South Australia 5034, Australia
P: 08-8373-4811 F: 08-8373-1053 C: 61
PERTH Unit 4, 36 Port Kembla Drive, Bibra Lake, Western Australia 6163, Australia
P: 089-434-1311 F: 089-434-1318 C: 61

China:

NSK HONG KONG LTD.
HONG KONG Room 512, Wing On Plaza, Tsim Sha Tsui East, Kowloon, Hong Kong
P: 2739-9933 F: 2739-9323 C: 852

KUNSHAN NSK CO., LTD.
KUNSHAN 258 South Huang Pu Jiang Rd Kunshan E&T Development Zone
Jiang Su P.R., 215335, China
P: 0520-7305654 F: 0520-7305689 C: 86

GUIZHOU HS NSK BEARINGS CO., LTD.
ANSHUN Dongjiao, Anshun, Guizhou, 561000, China
P: 0853-3521505 F: 0853-3522722 C: 86

NSK REPRESENTATIVE OFFICES
BEIJING Room 515, Beijing Fortune Bldg., 5 Dong san Huan Bei Lu, Chao Yang District, Beijing, 100004, China
P: 010-6590-8161 F: 010-6590-8166 C: 86
SHANGHAI Room 1005, Shanghai International Trade Center 2200 Yan An Road (w.), Shanghai, 200336, China
P: 21-6209-9051 F: 21-6209-9053 C: 86
GUANGZHOU Room 2701-02, Guangzhou International Electronics Tower 403, Huan Shi Rd East, Guangzhou, 510095, China
P: 020-8732-0583 F: 020-8732-0574 C: 86
ANSHUN Dongjiao, Anshun, Guizhou, 561000, China
P: 0853-3522522 F: 0853-3522552 C: 86

India:

RANE NASTECH LTD.
CHENNAI 14, Rajagopalan Salai, Vallancherry Guduvancherry, Pin-603 202, India
P: 04114-65313, 65314, 65365, 66002 F: 04114-66001 C: 91

NSK REPRESENTATIVE OFFICE
CHENNAI 2A, First Street, Cenotaph Road, Chennai, 600 018, India
P: 044-4334732 F: 044-4334733 C: 91

Indonesia:

P.T. NSK BEARINGS MANUFACTURING INDONESIA
JAKARTA PLANT Blok M-4, Kawasan Berikat, MM2100 Industrial Town Cibitung, Bekasi 17520, Jawa Barat, Indonesia
P: 021-898-0155 F: 021-898-0156, 021-898-0183 C: 62

Korea:

NSK KOREA CO., LTD.
SEOUL 9F (West Wing) Posco Center 892, Deachi 4 Dong Kangnam-Ku, Seoul, Korea
P: 02-3287-0300 F: 02-3287-0345, 0445 C: 82
CHANGWON PLANT 60, Songsan-Dong, Changwon, Kyungsangnam-Do, Korea
P: 0551-287-6001 F: 0551-285-9982 C: 82

Malaysia:

NSK BEARINGS (MALAYSIA) SDN. BHD.
KUALA LUMPUR 1st Floor, Kompleks Kemajuan, No.2, Jalan 19/1B, 46300 Petaling Jaya, Selangor Darul Ehsan, Malaysia
P: 03-7958-4396 F: 03-7958-4412 C: 60
PRAI 10, Lengkok Kikik 1, Taman Inderawasih, 13600 Prai, Penang, Malaysia
P: 04-399-1763 F: 04-399-1830 C: 60
JOHOR BAHRU Ground Floor, No. 27, Jalan Bakawali 50, Taman Johor Jaya, 81100 Johor Bahru, Johor, Malaysia
P: 07-354-6290 F: 07-354-6291 C: 60
KOTA KINABALU Lot 10, Lrg. Kurma 4, Likas Ind. Centre, 5 ½Miles, Jalan Tuaran, 88450 Inanam Sabah, Malaysia
P: 088-421-260 F: 088-421-261 C: 60

NSK MICRO PRECISION (M) SDN. BHD.
MALAYSIA PLANT No.43 Jalan Taming Dua,Taman Taming Jaya, 43300 Balakong, Selangor Darul Ehsan, Malaysia
P: 03-961-6288 F: 03-961-6488 C: 60

New Zealand:

NSK NEW ZEALAND LTD.
AUCKLAND 3 Te Apunga Place Mt. Wellington, Auckland, New Zealand
P: (09) 276-4992 F: (09) 276-4082 C: 64

Philippines:

NSK REPRESENTATIVE OFFICE
MANILA Unit 910 PS Bank Tower Sen. Gil Puyat Avenue Corner Tindalo Street, Makati City 1200, Metro Manila, Philippines
P: 02-759-6246 F: 02-759-6249 C: 63

Singapore:

NSK INTERNATIONAL (SINGAPORE) PTE LTD.
SINGAPORE 48 Toh Guan Road #04-02 Singapore 608837
P: (65) 273 0357 F: (65) 275 8937 C: 65

NSK SINGAPORE (PTE) LTD.
SINGAPORE 48 Toh Guan Road #02-03 Singapore 608837
P: (65) 278 1711 F: (65) 273 0253 T: RS24058 C: 65

Taiwan:

TAIWAN NSK PRECISION CO., LTD.
TAIPEI 9th Fl., 34, Chung Shan N. Rd., Sec. 3, Taipei, Taiwan R.O.C.
P: 02-2591-0656 F: 02-2597-3101 C: 886
TAICHUNG 107-6, SEC, 3, Wenxin Rd., Taichung, Taiwan R.O.C.
P: 04-311-7978 F: 04-311-2627 C: 886

Thailand:

NSK BEARINGS (THAILAND) CO., LTD.
BANGKOK 25th Floor RS Tower, 121/76-77 Rachadaphisek Road, Dindaeng, Bangkok 10320, Thailand
P: 02-6412150~58 F: 02-6412161 C: 66

NSK SAFETY TECHNOLOGY (THAILAND) CO., LTD.
CHONBURI Amata Nakorn Industrial Estate 700/68 Moo 6 Bangna-Trad Rd., T. Don-Hua-Roh A. Muang, Chonburi 20000, Thailand
P: (038) 214-317-8 F: (038) 214-316 C: 66

SIAM NASTECH CO., LTD.
CHACHOENGSAO 90 Moo 9, Wellgrow Industrial Estate, Km. 36 Bangna-Trad Road, Bangwao, Bangpakong, Chachoengsao 24180, Thailand
P: (038) 522-343~350 F: 038-522-351 C: 66

Europe

NSK EUROPE LTD. (EUROPEAN HEADQUARTERS)
RUDDINGTON, UK Mere Way, Ruddington, Nottinghamshire, NG11 6JZ U.K.
P: 0115-936-6464 F: 0115-936-6400 C: 44

France:

NSK FRANCE S.A.
PARIS Quartier de l'Europe, 2 Rue Georges Guynemer, 78283 Guyancourt Cedex, France
P: (01) 30-57-39-39 F: (01) 30-57-00-01 T: 698578 C: 33
LYON Immeuble "Le Périphérique" 16, Rue des Bosses, 69623 Villeurbanne Cedex, France
P: (04) 72-15-29-00 F: (04) 72-37-54-03 C: 33

Germany:

NSK DEUTSCHLAND GMBH
DÜSSELDORF Harkortstr. 15, 40880 Ratingen, Germany
P: 02102-481-0 F: 02102-481-229 C: 49
STUTTGART Sielminger Str. 65, 70771 Leinfelden-Echterdingen, Germany
P: 0711-79082-0 F: 0711-79082-499 C: 49
LEIPZIG Zschortauer Str. 76, 04129 Leipzig, Germany
P: 0341-5631241 F: 0341-5631243 C: 49

NEUWEG FERTIGUNG GMBH
CORPORATE Ehinger Strasse 5, D-89593 Munderkingen, Germany
OFFICE/PLANT P: 07393-540 F: 07393-3732 C: 49

Italy:

NSK ITALIA S.P.A.
MILANO Via XX Settembre, 30 20024 Garbagnate Milanese (Milano), Italia
P: 02-995-191 F: 02-99025778, 02-99028373 C: 39

Poland:

NSK EUROPE LTD. WARSAW LIAISON OFFICE
WARSAW LIAISON OFFICE Oddzial w Warszawie, ul. Migdalowa 4 lok. 73, 02-796 Warsaw, Poland
P: 48-22-645-1525, 1526 F: 48-22-645-1529 C: 48

NSK ISKRA S.A.
CORPORATE Ul. Jagiellońska 109, 25-734 Kielce, Poland
OFFICE/PLANT P: 48-41-366-6111 F: 48-41-345-4599 C: 48

Spain:

NSK SPAIN S.A.
BARCELONA Calle de la Hidráulica, 5, P.I. "La Ferreria" 08110 Montcada i Reixac (Barcelona), Spain
P: 93-575-4041 F: 93-575-0520 C: 34

Switzerland:

WAELZLAGER INDUSTRIEWERKE BULLE AG (W.I.B.)
CORPORATE Rue Champ-Barby 25, Ch-1630 Bulle, Switzerland
OFFICE/PLANT P: 026-9191100 F: 026-9191120 C: 41

Turkey:

NSK BEARINGS MIDDLE EAST TRADING CO., LTD.
ISTANBUL Eski Uskudar Cad. Cayir Yolu Sok. Nora Center Kat 1, 81090 Icerenkoy, Istanbul, Turkey
P: 90-216-463-61-50 F: 90-216-463-61-47 C: 90

United Kingdom:

NSK BEARINGS EUROPE LTD.
GROUP Northern Road, Newark, Nottinghamshire, NG24 2JF U.K.
OFFICE P: 01636-605123 F: 01636-642083 T: 377652 C: 44
PETERLEE PLANT 3 Brindley Road, South West Industrial Estate, Peterlee, Co. Durham, SR8 2JD U.K.
P: 0191-586-6111 F: 0191-586-3482 C: 44
FORGE PLANT Davey Drive, North West Industrial Estate, Peterlee, Co. Durham, SR8 2PW U.K.
P: 0191-518-0777 F: 0191-518-0303 C: 44
NEWARK PLANT Northern Road, Newark, Nottinghamshire, NG24 2JF U.K.
P: 01636-605123 F: 01636-605000 T: 377652 C: 44
BLACKBURN PLANT Roman Road Industrial Estate, Blackburn, Lancashire, BB1 2LZ U.K.
P: 01254-661921 F: 01254-679502 C: 44
AEROSPACE PLANT/SALES Oldends Lane, Stonehouse, Gloucestershire, GL10 3RH U.K.
P: 01453-822333 F: 01453-825945 C: 44

NSK EUROPEAN TECHNOLOGY CO., LTD.
RUDDINGTON Mere Way, Ruddington, Nottinghamshire, NG11 6JZ U.K.
P: 0115-940-5409 F: 0115-940-5419 C: 44

NSK UK LTD.
RUDDINGTON Mere Way, Ruddington, Nottinghamshire, NG11 6JZ U.K.
P: 0115-936-6600 F: 0115-936-6702 C: 44

NSK STEERING SYSTEMS EUROPE LTD.
CORPORATE Gallagher Business Park, Silverstone Drive, Rowleys Green, Coventry, CV6 6PA U.K.
OFFICE/PLANT P: 024-76-710300 F: 024-76-710599 C: 44
PETERLEE PLANT 1 Palmer Road, South West Industrial Estate, Peterlee, Co. Durham, SR8 2JJ U.K.
P: 0191-518-6800 F: 0191-518-6808 C: 44
PETERLEE EPS PLANT 7 Doxford Drive, South West Industrial Estate, Peterlee, Co. Durham, SR8 2RL U.K.
P: 0191-518-6400 F: 0191-518-6440 C: 44

North and South America

NSK AMERICAS, INC. (AMERICAN HEADQUARTERS)
ANN ARBOR, USA 3861 Research Park Drive, Box 1507, Ann Arbor, Michigan 48106-1507, U.S.A.
P: 734-761-9500 F: 734-761-9511 C: 1

Argentina:

NSK ARGENTINA SRL
Av. Córdoba, 659-1° Piso-Oficinas 13/14-Buenos Aires-Argentina
P: 011-4315-1322 F: 011-4312-7644 C: 54

Brazil: www.nsk-ltd.com.br

NSK BRASIL LTDA.
SÃO PAULO Rua 13 de Maio, 1633-14°. Andar-Bela Vista-CEP 01327-905-São Paulo-SP, Brazil
P: 011-269-4723 F: 011-269-4720 C: 55
PORTO ALEGRE Av. Cristovão Colombo, 1694-1° Andar-Sala 201-Floresta, CEP 90560-001, Porto Alegre, RS, Brazil
P: 051-222-1324 F: 051-222-2599 C: 55
BELO HORIZONTE Rua Ceará, 1431-4° Andar-Sala 405-Funcionários-CEP 30150-311, Belo Horizonte, MG, Brazil
P: 031-274-2477 F: 031-273-4408 C: 55
JOINVILLE Rua Mário Lobo, 61-11° Andar-Sala 1112-Centro-CEP 89201-330, Joinville, SC, Brazil
P: 047-422-5445 F: 047-422-2817 C: 55
RECIFE Av. Conselheiro Aguiar, 2738-6° Andar-Conj. 604-Boa Viagem-CEP 51020-020, Recife, PE, Brazil
P: 081-326-3781 F: 081-326-5047 C: 55
SUZANO PLANT Av. Vereador João Batista Fitipaldi, 66, CEP 08685-000-Vila Maluf, Suzano, SP, Brazil
P: 011-7701-4007 F: 011-4748-2355 C: 55

Canada:

NSK CANADA INC.
HEAD OFFICE 5585 McAdam Road, Mississauga, Ontario L4Z 1N4, Canada
P: 905-890-0740 F: 905-890-0434 C: 1
MONTREAL 2150-32E Avenue, Lachine, Quebec H8T 3H7, Canada
P: 514-633-1220 F: 514-633-8164 C: 1
TORONTO 5585 McAdam Road, Mississauga, Ontario L4Z 1N4, Canada
P: 905-890-0561 F: 905-890-1938 C: 1
EDMONTON 9267-41st Avenue, Edmonton, Alberta T6E 6R5, Canada
P: 604-294-1151 F: 604-294-1407 C: 1
VANCOUVER 3353 Wayburne Drive, Burnaby, British Columbia V5G 4L4, Canada
P: 604-294-1151 F: 604-294-1407 C: 1

Mexico:

NSK RODAMIENTOS MEXICANA, S.A. DE C.V.
MEXICO CITY Minas Palacio No.42-6, Col. San Antonio Zomeyucan Naucalpan de Juarez, C.P. 53750 Estado de Mexico, Mexico
P: 5-301-2741, 5-301-3115, 5-301-4762 F: 5-301-2244, 5-301-2865 C: 52

United States of America: www.nsk-corp.com

NSK CORPORATION
[CORPORATE OFFICE, Aftermarket Business Unit, OEM Business Unit]
ANN ARBOR 3861 Research Park Drive, Box 1507, Ann Arbor, Michigan 48106-1507, U.S.A.
P: 734-761-9500 F: 734-761-9511, 734-668-7888 C: 1

[BRANCHES and DISTRIBUTION CENTERS]
LOS ANGELES 13921 Bettencourt Street, Cerritos, California 90703, U.S.A.
P: 562-926-2975 F: 562-926-3553 C: 1
SAN JOSE 1900 McCarthy Boulevard, Suite 107, Milpitas, California 95035, U.S.A.
P: 408-944-9400 F: 408-944-9405 C: 1
INDIANAPOLIS 5550 Progress Road, Park Fletcher, Indianapolis, Indiana 46241, U.S.A.
P: 317-247-4724 F: 317-247-5660 C: 1
ATLANTA 5575 Gwaltney Drive, Atlanta, Georgia 30336, U.S.A.
P: 404-349-2888 F: 404-349-1209 C: 1

[PLANTS]
ANN ARBOR 5400 South State Road, Box 990, Ann Arbor, Michigan 48108, U.S.A.
P: 734-996-4400 F: 734-996-4707 C: 1
CLARINDA 1100 N First Street, Clarinda, Iowa 51632, U.S.A.
P: 712-542-5121 F: 712-542-4905 C: 1
FRANKLIN 3400 Bearing Drive, Franklin, Indiana 46131, U.S.A.
P: 317-738-5000 F: 317-738-4310 C: 1
LIBERTY 1112 East Kitchel Road, Liberty, Indiana 47353, U.S.A.
P: (765) 458-5000 F: (765) 458-7832 C: 1

NSK AMERICAN TECHNICAL CENTER
ANN ARBOR 3917 Research Park Drive, Ann Arbor, Michigan 48108, U.S.A.
P: 734-668-0877 F: 734-668-0852 C: 1

NSK PRECISION AMERICA, INC.
CHICAGO 250 Covington Drive, Bloomingdale, Illinois 60108, U.S.A.
P: 630-924-8000 F: 630-924-8197 C: 1

NASTECH
CORPORATE 110 Shields Drive Route 2, Box 0030, Bennington, Vermont 05201-8309, U.S.A.
OFFICE/PLANT P: 802-442-5448 F: 802-442-2253 C: 1
SALES OFFICE 2851 Boardwalk Drive, Ann Arbor, Michigan 48104, U.S.A.
P: 734-669-8272 F: 734-669-8102 C: 1

NSK LATIN AMERICA INC. www.nsk-corp.com/miami
MIAMI 2500 NW 107 Avenue, Suite 300, Miami, Florida, 33172, U.S.A.
P: (305) 261-7824 F: (305) 261-6246, (305) 267-7447 C: 1

P: Phone F: Fax T: Telex C: Country Code

Printed in Japan

Motion & Control

No.10 April 2001

Published by NSK Ltd.